NEW MEXICO BUREAU OF GEOLOGY AND MINERAL RESOURCES
Open-File Report 629 2024

Yardangs at White Sands National Park, New Mexico, USA

Steven G. Fryberger and Charles F. Fryberger

OPEN-FILE REPORT

Open-File Report 629—Yardangs at White Sands National Park, New Mexico, USA

S.G. Fryberger, Department of Earth Sciences, Denver Museum of Nature & Science, 2001 Colorado Blvd., Denver, CO 80205

C.F. Fryberger, Sparkshop LLC, 5070 Benton Way, Denver, CO 80212

New Mexico Bureau of Geology and Mineral Resources
A research and service division of New Mexico Institute of Mining and Technology

Copyediting: Frank Sholedice

Layout: Lauri Logan

Publications Program Manager: Barbara J. Horowitz

Cover Photograph: A large yardang with a typical blunt prow (on the left) that tapers downwind to a narrower stern. The steep cross-bedding within the yardang indicates that it was sculpted in large part from lightly indurated slipface deposits of a dune. Cross-bedding dips mostly to the right, recording the southwesterly wind direction that first deposited the original dune and later sculpted the yardang. View toward the north. Co-author Charles Fryberger provides scale. *Photo by Steven Fryberger*

Suggested Citation: Fryberger, S.G., and Fryberger, C.F., 2024, Yardangs at White Sands National Park, New Mexico, USA: New Mexico Bureau of Geology and Mineral Resources Open-File Report 629, 50 p.
https://doi.org/10.58799/OFR-629

ACKNOWLEDGMENTS

Many thanks to Wes Ward for providing a copy of his classic 1984 paper, co-authored by Ron Greeley, at Rogers Dry Lake that provided important comparative data for our study at White Sands, as well as his original photographs from Rogers Dry Lake and his sage counsel on Martian yardangs. From Jim Zimbelman we received great guidance and encouragement, as well as help with the literature on Martian yardangs. We thank the White Sands National Park staff who accompanied us in fieldwork on many occasions, including long hikes to relatively remote places in the park and the missile range. John Mangimeli of the National Park Service at White Sands provided encouragement over the years of our field research. The U.S. Air Force provided a helicopter flight over White Sands that yielded useful photographs. Also, thanks to Google Earth for the space imagery (including the Google Mars imagery) that helped this study immensely. We thank Rip Langford for his helpful discussions and ideas on the ancient shorelines of Lake Otero, as well as his thoughtful critique of an early draft of this paper. Thanks to Bruce Allen for helpful comments on lacustrine shorelines at White Sands and Lake Estancia and related process frameworks at White Sands. We also thank Shari Kelley, Frank Sholedice, Lauri Logan, and Franci Fryberger for their editorial skills, which contributed greatly to the readability of this report.

CONTENTS

Figures

Table

ABSTRACT

Yardangs are streamlined geomorphic features created by eolian erosion of indurated sediments, non-sedimentary bedrock, or other wind-erodible material. In this study, we document the distribution, types, and sizes of yardangs present at White Sands National Park, New Mexico, using fieldwork and satellite imagery. The recognition and documentation of these yardangs is important because wind erosion and its products have created much of the geomorphology of White Sands. Understanding the wind erosion events recorded by the White Sands yardangs may also shed light on the processes and history of the preservation and subsequent exposure of the ancient human footprints recently discovered on the Alkali Flat. Additionally, the yardangs of White Sands provide possible analogs for yardangs on Mars.

There are three types of yardangs at White Sands. They are informally referred to here as *scarp, bedform,* and *shrub* yardangs based on their depositional setting and processes of formation. *Scarp yardangs* are mostly formed from moderately indurated, gypsiferous sediments of ancient Lake Otero. These yardangs are commonly developed as retreating scarps along paleoshorelines of Lake Otero or downwind of the shallow, wind-eroded basin on the Alkali Flat. *Bedform yardangs* are formed from sediments of dunes and associated facies such as interdunes, sand sheets, and sabkhas. At White Sands, these yardangs are derived from sediments that have undergone early cementation. *Shrub yardangs* at White Sands are formed by the erosion and streamlining (most commonly) of indurated eolian dune sediments hosting *Tamarix* spp. or other shrubs.

Our measurements using satellite imagery document a wide range of sizes and shapes for yardangs at White Sands, few of which fit the ideal 1:4 ratio of width to length (W:L) in situations of ideal streamlining. Additionally, the yardangs at White Sands have clear shape differences among and within types.

The yardangs at White Sands are closely aligned with the resultant drift direction of the wind regime at Holloman Air Force Base (064°, or toward the northeast). Sand roses constructed from the wind records at Holloman indicate a dominant wind from the southwest during most months. Subsidiary modes exist as well, comprising winds from the northwest (winter) and southeast (summer). The yardangs at White Sands have formed in a low- to moderate-energy wind regime. This process may have been possible due to the generally weak induration of the sediments. It is common at White Sands for the interfluves along wind-eroded scarps to be streamlined by wind to form yardangs. The yardangs tend to translate downwind as the sediments are stripped away.

Most yardangs at White Sands are carved from dominantly gypsiferous sediments of fluvial, lacustrine, or eolian origin. The cohesion required to form yardangs commonly occurs because the sediments have been cemented by (a) precipitation of evaporite cements in proximity to a saline groundwater table, (b) dissolution and reprecipitation of gypsum by meteoric waters, or (c) precipitation of evaporite cements (mainly gypsum) around plant roots or rhizomes.

Ponded water at Lake Lucero in foreground, with channel and white gypsum evaporites beyond. In the distance, the modern highstand shoreline and San Andres Mountains. *Photo by Steven Fryberger*

PREVIOUS STUDIES

Previous studies of yardangs that contributed directly to this report fall into two broad categories. Early studies were undertaken by scientists whose main interest was the geological and climatic history of Earth. Later studies have been conducted with an eye toward interpretation of similar features on Mars.

EARLY CLASSIC WORK

Hedin (1905) proposed the term "yardangs" for landscape features he observed during his travels in Chinese Turkestan. Bosworth (1922) worked in northwestern Peru, studying Tertiary and Quaternary sediments. He did not use the term "yardangs" but published many photos and drew a comparison with inverted boat hulls that is now commonly used to describe yardang geomorphology. Blackwelder (1934) authored a classic study of yardangs at Rogers Dry Lake that, among others such as Ward and Greeley (1984), has guided our work at White Sands.

YARDANGS IN THE GEOLOGICAL RECORD

Few studies have identified ancient yardangs in the geological record. One suspects, however, that there are more yardangs preserved in the rock record than previously identified as such simply because yardangs are so common on Earth today. Tewes and Loope (1992) identified yardangs in the White Rim Formation at Canyonlands National Park, Utah, USA. Jones and Blakey (1993) recognized possible yardangs at the boundary between the Page and Carmel Formations in Utah.

YARDANG SYSTEMS ON EARTH

McCauley et al. (1977a, 1977b, 1979) wrote a series of expeditionary reports on yardangs and other eolian features in Egypt and Peru. McCauley also suggested the concept of an "eolian takeover of the landscape" from previously dominant fluvial processes during transitions from wet to dry climates—an idea that has proven powerful as an interpretative tool on both Earth and Mars. El-Baz et al. (1979), Breed et al. (1980, 1982, 1989), Grolier et al. (1980), and Whitney (1985) studied the dunes and yardangs of Egypt, a country that has many sizes and shapes of yardangs (and dunes) that invite comparison with Mars. El-Baz (2001) provided a popular review pointing out the similarity of the Great Sphinx of Giza near Cairo to yardangs seen in the Egyptian desert. Brook (2002) described interesting small yardangs in Somalia that are similar to those at White Sands (see his fig. 3, p. 145). Gutiérrez-Elorza et al. (2002) described extensive yardang fields in the Ebro depression of Spain that have formed in a closed basin setting similar to the Tularosa Basin of White Sands. Ritley and Odontuya (2004) described small yardangs in Mongolia similar in some ways to those at White Sands (see their fig. 2). Goudie (2007, 2008) provided wide-ranging global reviews of yardangs that were very helpful to us. Laity (2009) also published an overview of yardangs worldwide. In a step toward the classification of yardangs, she noted three types: micro-yardangs (centimeter-scale ridges), meso-yardangs (several meters high and long), and mega-yardangs (tens of meters high and kilometers long). Each size class of yardangs has associated sediments and process frameworks. De Silva et al. (2010) described yardangs in ignimbrites in Bolivia that are direct analogs for those on Mars. Sebe et al. (2011) mapped extensive yardangs in the Pannonian Basin of Central Europe. Ghodsi (2017) described the famous yardangs cut into alluvial deposits in the Lut Desert of Iran, without which no discussion of yardangs is complete. Pelletier et al. (2018) provided a superb and very comprehensive description of yardangs near the Salton Sea, California, USA, that included flux measurements and a discussion of process frameworks for the evolution of yardangs in areas with folded rocks (see their figs. 3 and 7). Favaro et al. (2021) identified controls on yardang

morphology in the Campo de Piedra Pómez ignimbrites of northwestern Argentina, where bands of yardangs are controlled by preexisting antecedent topography in the bedrock, such as fumaroles or ridges associated with pyroclastic flow deposits.

There are excellent contributions from Chinese scientists studying yardangs in northwestern China. Among the most useful papers for this report is that of Li et al. (2016), who identified various morphological types of yardangs and associated process frameworks. Also of interest are contributions by Hu et al. (2017), who showed that yardang geometries in the Qaidam Basin are mainly controlled by the structural geology and rheology of the sedimentary rocks from which they were formed. Wang et al. (2018) studied the Qaidam Basin yardangs of northwestern China and classified them into 11 different types within four main groups. Xuemin et al. (2019) reported that long-ridge yardang formation seems to require strong, unidirectional winds in high- or intermediate-energy wind environments. Zhang et al. (2020) showed that gravel layers among fine-grained sediments were gradually exposed by wind, slowing both the deflation forming the yardangs and the contribution of dust to the Pacific Ocean. Ding et al. (2020) discuss Earth yardangs and compare them to yardangs on Mars. Of particular interest is their figure 4 on page 6, which shows an evolutionary model for the growth and maturity (morphological evolution) of yardangs.

YARDANG SYSTEMS ON MARS

McCauley (1973) provided an early description of wind erosion on Mars from Mariner 9 imagery. Ward (1979) provided a thorough description of yardangs on Mars, interpreting them as products of relatively recent wind erosion. Ward et al. (1985) also published a comprehensive map of eolian features on Mars that included yardangs as well as dunes. Breed et al. (1989) mapped the type and distribution of dunes on Mars. Although not specifically about yardangs, their study is very useful because the dunes on Mars provide a confirmation of local wind direction.

Szynkiewicz et al. (2010) compared Earth gypsum dunes at White Sands with Martian gypsum dunes of the Olympia Undae dune field (north polar region). Kerber and Head (2010) described yardangs in the Martian Medusae Fossae Formation, including an evolutionary sequence of crater erosion forming yardangs. Zimbelman and Griffin (2010) analyzed the superb HiRISE images of yardangs in the equatorial Medusae Fossae Formation.

BACKGROUND AND OVERVIEW OF THE PRESENT STUDY

The authors undertook substantial fieldwork at White Sands with Chris Schenk of the U.S. Geological Survey and with White Sands staff and volunteers during the 1990s and early 2000s. This earlier work was part of a study of the eolian sedimentology of White Sands, with emphasis on the early cementation of the gypsum sands (Schenk and Fryberger, 1988). The geology of White Sands was summarized in several documents, including Fryberger (2001a, 2001b) and Fryberger and Ormerod (2023). These works provide a brief overview of the yardangs at White Sands. The present, more complete study of the yardangs at White Sands fills the gaps in our knowledge of the types of yardangs and their distribution, size, and formative processes.

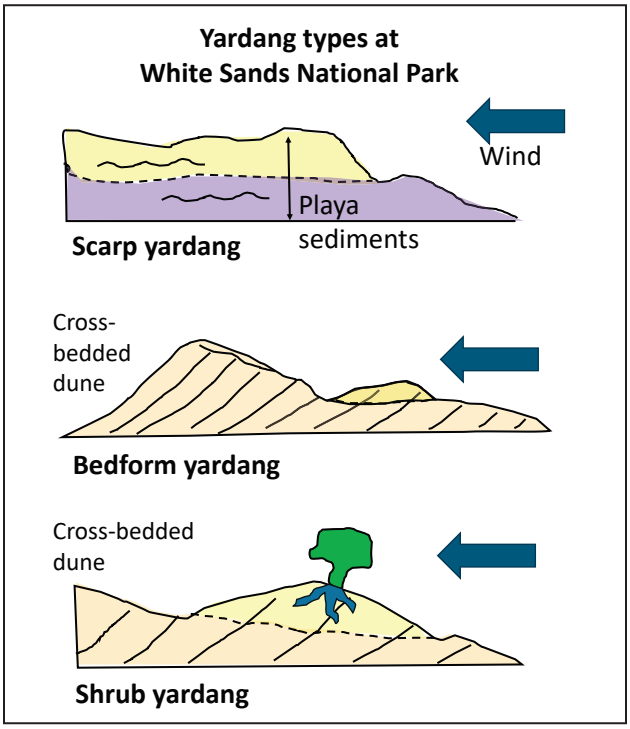

Figure 1. Typical settings where yardangs (shaded yellow) form at White Sands. The basic process of formation—wind scour of indurated sediment—is the same for all three. Labels show the associated scarp, bedform, and shrub yardang types.

We recognize three types of yardangs at White Sands (Fig. 1), classified mainly on the substrate from which they are carved and the process frameworks in which they are formed. These are scarp, bedform, and shrub yardangs (Figs. 1–3).

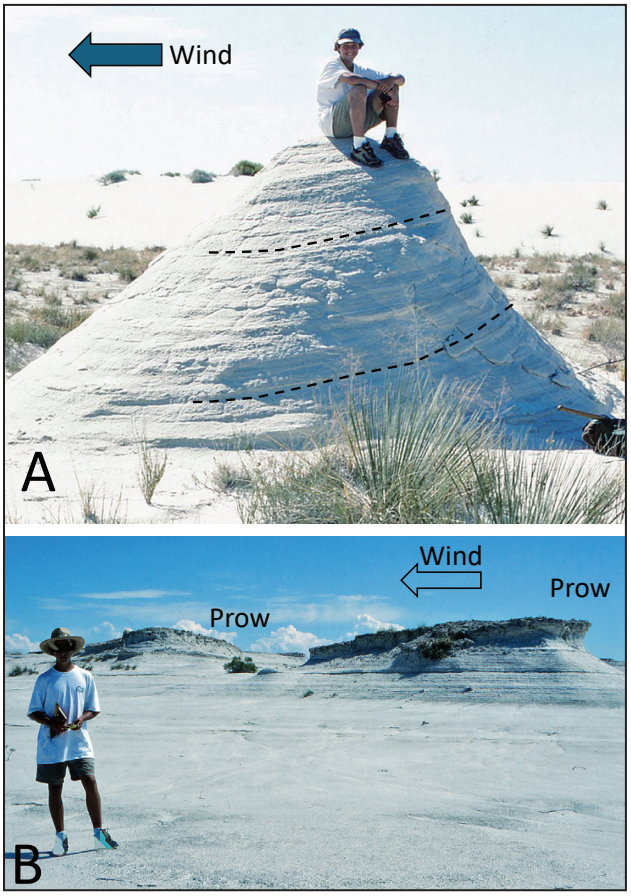

Figure 2. Bedform and scarp yardangs. (A) A bedform yardang within the parabolic dune field that extends northeast of the southern end of Lake Lucero. This compact, well-streamlined morphology is common among bedform yardangs. Eolian cross-bedding dips to the left (dashed lines). Note steeper slope on upwind (right) side of the yardang. (B) An oblique view of the prows of two scarp yardangs along the southern shoreline of Lake Lucero. Flat gypsum bedding of a Lake Otero evaporitic phase (playa phase, in other words) is visible beneath the case-hardened top of the yardang.

Scarp yardangs (top of Fig. 1) are typically formed from resistant scarps along the old shorelines of Lakes Otero and Lucero. At White Sands, they are usually carved from lacustrine (playa) sediments. There is commonly a wind-resistant cap of cemented or case-hardened, coarse gypsum crystals on the yardang. These yardangs shift downwind as the scarp retreats due to wind and fluvial erosion. Bedform yardangs (center of Fig. 1) are commonly formed from indurated dune sediments. They also form from indurated sediments of interdune, sand sheet, or eolian sabkha sediments. These yardangs gradually erode and disappear as the dune moves on and the cemented zone is scoured away. Shrub yardangs (bottom of Fig. 1) are created where sand has become cemented around plant roots or rhizomes, then eroded by wind. Shrub yardangs, being dependent upon an immobile plant such as *Yucca* spp. (yucca) or *Tamarix* spp. (saltcedar), are stationary, gradually eroding in place after forming by wind scour.

The informal types of yardangs we recognize at White Sands fit into broad "global" categories that relate to their origin, manner of evolution, and shape; these are stationary, translational, and extensional yardangs (Fig. 4).

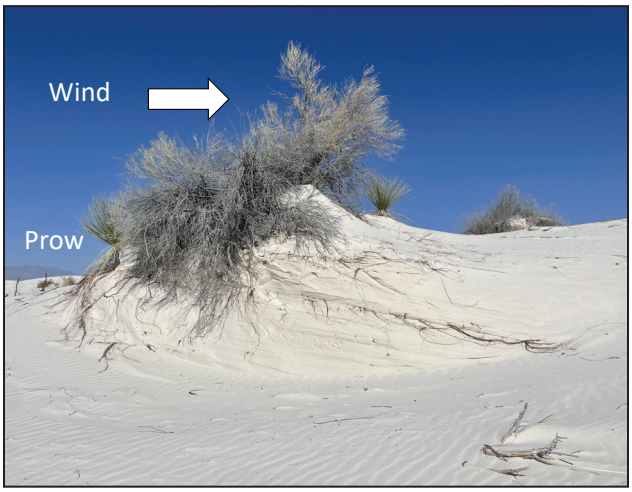

Figure 3. A shrub yardang, sometimes referred to locally as a "pedestal dune." It is streamlined downwind of the saltcedar shrub that protects the upwind prow. Exposed cross-bedding is from a dune that has migrated downwind. Most shrub yardangs illustrated in this report did not originate due to trapping of windblown sand by vegetation to form a streamlined shape. Rather, these yardangs are erosional features formed from previously cemented sand, whether as a dune or other eolian facies, on which the plant happened to grow. The cementation commonly occurred where gypsum was precipitated from an evaporitic groundwater table, or by the action of meteoric water that partly dissolved gypsum sand grains, then reprecipitated the gypsum upon evaporation.

At White Sands, the bedform (meaning dune bedforms as well as associated facies of interdune, sand sheet, or sabkha) and shrub yardangs belong in the stationary class for the most part. This is specifically because, at White Sands, they most commonly evolve from cemented portions of eolian dunes that migrate downwind, leaving the yardang behind. As the dune migrates onward, the wind streamlines, then gradually erodes away the yardang. At White Sands, yardangs formed on retreating scarps are translational. This is because yardang prows migrate downwind as the scarp erodes, commonly through a combination of fluvial and wind erosion, and because the yardangs are relatively short in length. The term "extensional" applies to yardangs that grow more by extension than vertically, sometimes for many kilometers downwind.

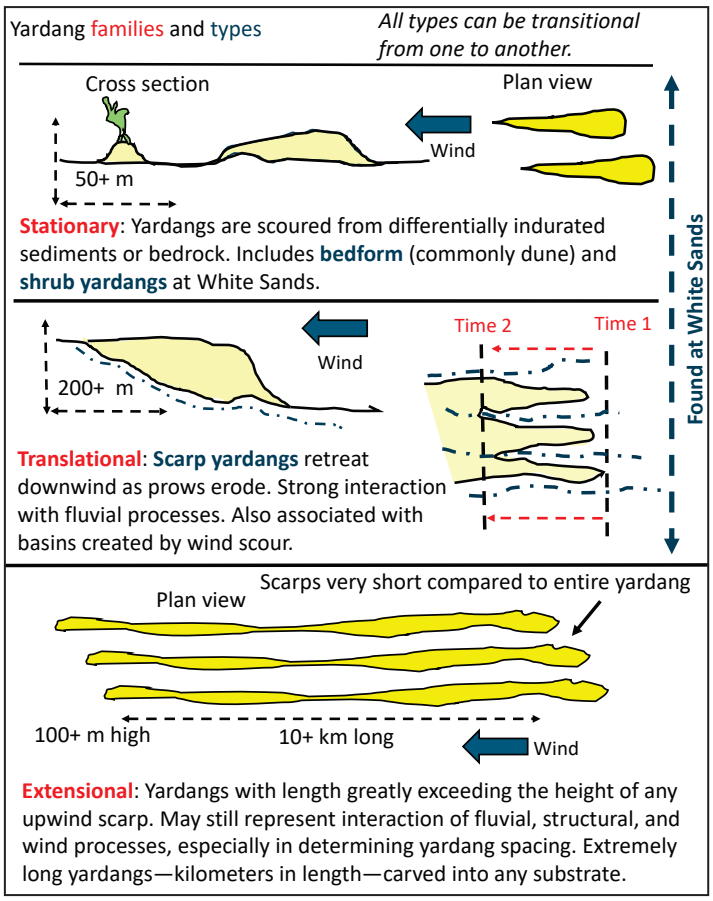

Figure 4. Morphological yardang types at White Sands and the "global" families into which they fit. At White Sands, the bedform, shrub, and scarp yardangs that we studied fell into only the first two of the broad families we observe worldwide—the stationary and translational types. The truly extensional yardangs, that is "long ridge" or "mega-yardangs," such as those in the Lut Desert of Iran, are not present at White Sands. The various types are transitional from one to another. We recognize, however, that there are many other ways to classify yardangs than the simple scheme outlined here.

Such yardangs are not present at White Sands but are widespread in some desert regions, such as the Lut Desert of Iran (Ghodsi, 2017).

The description of yardangs at White Sands adds to a terrestrial database that invites direct comparison with Martian yardangs—for example, those along retreating scarps, which is a phenomenon common at White Sands and on Mars (Fig. 5; see also Ding et al. [2020]).

The yardangs at White Sands document a relatively recent interval of the long history of wind erosion of the Alkali Flat at White Sands—a process that continues in the present day. The timing and processes of wind erosion of the Alkali Flat, as well as the various terrains sculpted into yardangs, may have application to discussions of the ancient human footprints found on the Alkali Flat in recent years (Bustos et al., 2018; Bennett et al., 2019, 2020, 2021). In addition, knowledge of the process frameworks contributing to the development of yardangs may assist with resource management at White Sands. This is especially relevant regarding the short- and long-term effects of the level of the water table on wind erosion and deposition, a process with ties to the formation of yardangs in the park.

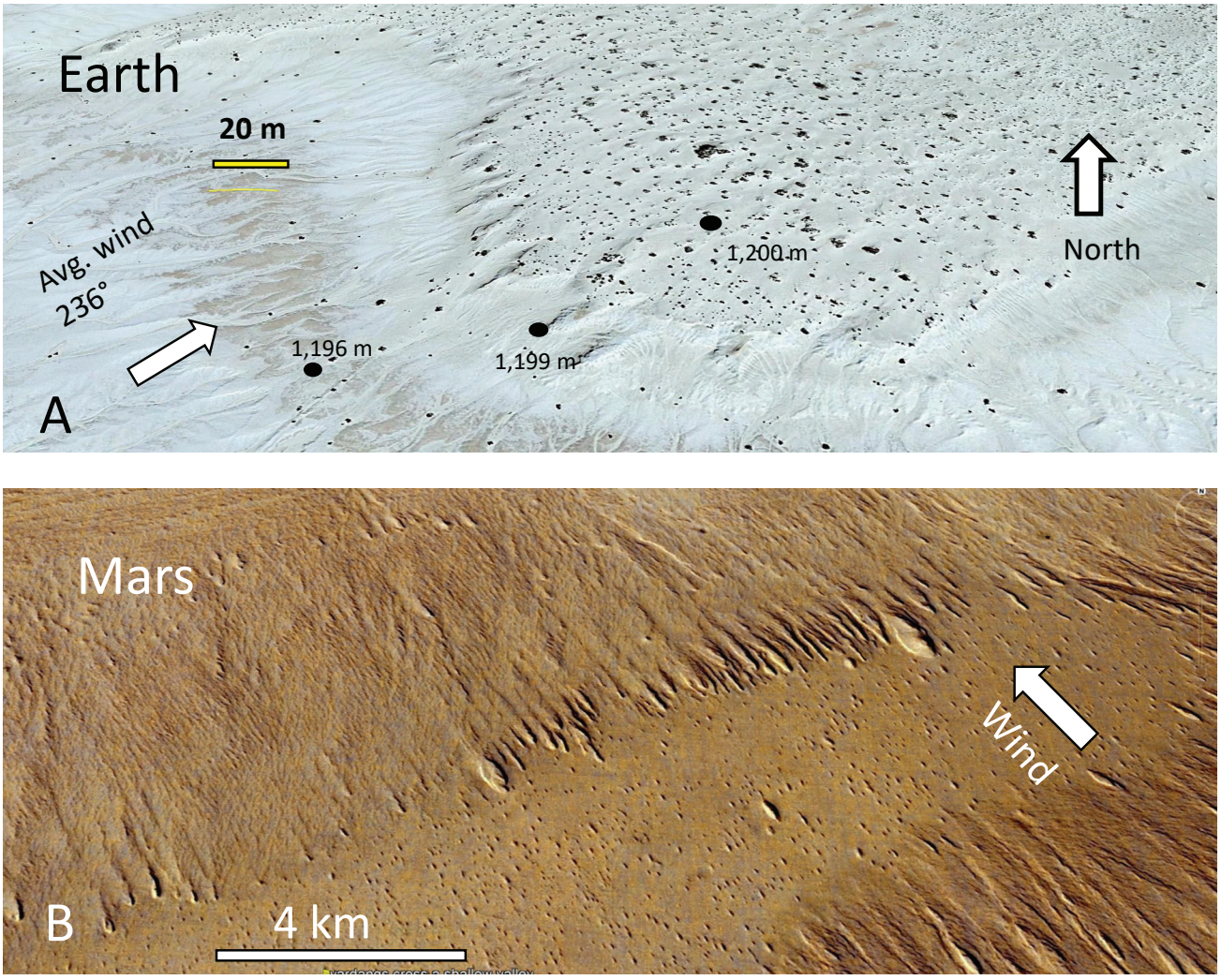

Figure 5. A comparison of yardangs at White Sands with those on Mars. (A) A satellite image of the northern part of the White Sands dune field. This view shows yardangs formed from interfluves along a scarp eroded by wind, mainly from Lake Otero sediments. The yardangs are closely aligned with the dominant wind from the southwest. Shallow gullies are present on the sides of these emerging yardangs, a few of which are distinct topographically from the plateau to the east. The black dots mark spot elevations. (B) Yardangs from the Elysium Planitia region of Mars. Note the sawtooth scarp yardangs formed as the ridge was eroded by wind. The similarity to those from White Sands is striking. Vertical exaggeration in both figures is 3×. Both images are courtesy of Google Earth.

GEOLOGICAL SETTING OF WHITE SANDS

The study area at White Sands National Park is in the southwestern United States, within the Rio Grande rift (Fig. 6). Geologically youthful volcanism and the extensional tectonics of the Rio Grande rift have configured the present bedrock topography and drainage patterns of the region. The present situation, of course, is merely the latest phase of a long and complex geological history with direct bearing on the origins of White Sands and, thus, the yardangs of this study. A review of the geological history of the Tularosa Basin, in which White Sands National Park is located, is beyond the scope of this study. However, a full discussion is available in Fryberger and Ormerod (2023).

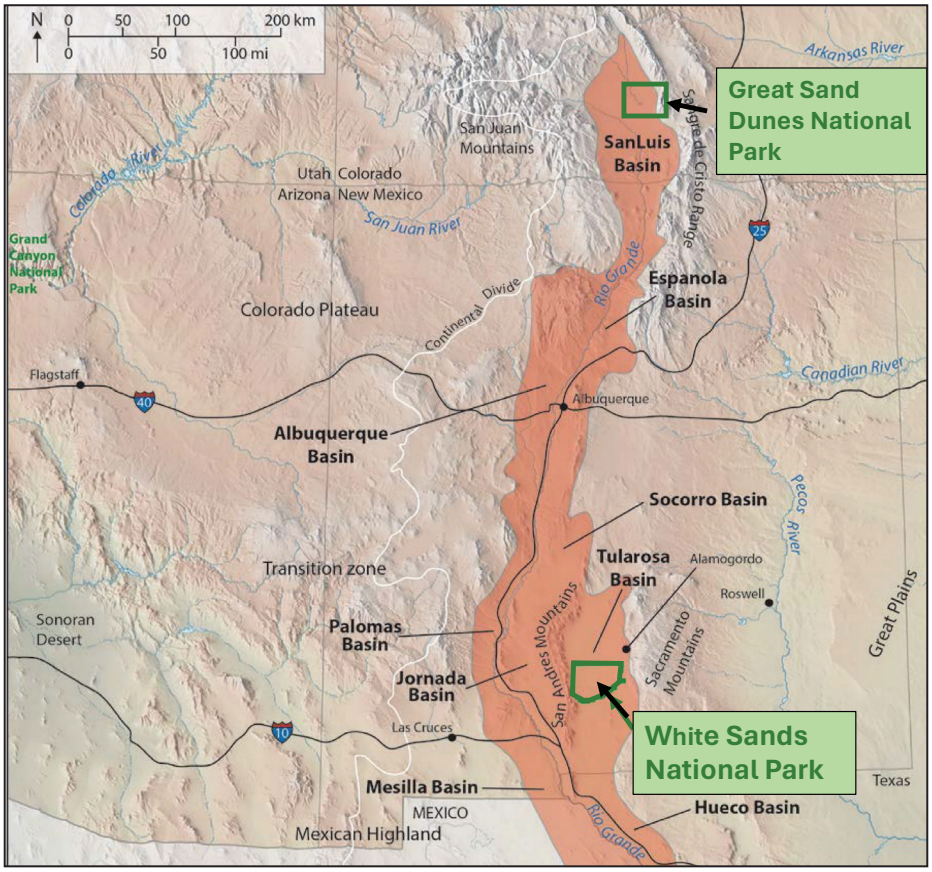

Figure 6. The Rio Grande rift of New Mexico and Colorado (shaded orange). This rift zone and its subbasins host large, active dune fields, such as Great Sand Dunes and White Sands, as well as extensive eolian sand sheets and smaller dune fields on the flanks of uplifts and drainages. After KellerLynn (2012); based on maps by Trista Thornberry-Ehrlich (Colorado State University), Tom Patterson (National Park Service), and Connell et al. (2005).

PREVIOUS WORK ON THE SURFICIAL GEOLOGY OF WHITE SANDS

GEOLOGY AND HYDROLOGY

Herrick (1904) named Lake Otero. Kottlowski (1958) provided a thorough explanation of the origins of the gypsum that constitutes the dunes at White Sands (recycled Permian evaporites). McLean (1970) described Tularosa Basin groundwater resources. Allmendinger (1971, 1972) and Allmendinger and Titus (1973) wrote the definitive account of the hydrology of Lake Lucero. Seager et al. (1987) published a geologic map covering White Sands and surrounding areas. Basabilvazo and Myers (1994) summarized the geohydrology of the laser test area on the Alkali Flat. Buck (1996) described a somewhat overlooked area of quartz sand dunes and sand sheet that lies immediately south of the more famous gypsum dunes at White Sands. Langford (2003) proposed and mapped several important Lake Otero shorelines. In a series of papers, Allen (1994, 2005), Allen and Anderson (2000), and Allen et al. (2006, 2009) described the sediments and lacustrine histories of Lake Estancia and Lake Otero. Lake Estancia, which lies roughly 160 miles north of White Sands, is a well-documented analog in many ways for Lake Otero at White Sands. Allen et al. (2009) described shoreline deposits of Lake Otero, provided dates on Pleistocene–Holocene outcrops of the sediments, and proposed an ultimate highstand at 1,204 m for Lake Otero. Fryberger (2001a, 2001b) and Fryberger and Ormerod (2023) published a geomorphic map and summary of the geology of White Sands as a website. A separate contribution by Fryberger included his geomorphic map of White Sands as part of the National Park Service White Sands Geologic Resources Inventory of KellerLynn (2012). Connell et al. (2005) documented Cenozoic drainage development in the Tularosa Basin. Langford et al. (2009) described groundwater salinity controls on dune type. Ewing (2010, 2020) provided an early study of the morphological evolution of the White Sands dune field and a later review of the evolution of White Sands as a whole. Baitis et al. (2014) discussed various models for the evolution of shorelines and dunes. Kocurek et al. (2007) described dune dynamics and water table controls on sedimentation. Newton and Allen (2014) conducted a study of the hydrology of groundwater and lake levels at White Sands (see their figure 37).

EOLIAN SEDIMENTOLOGY

Talmadge (1933) was among the first to suggest that gypsum from the Permian Yeso Formation contributed to the growth of White Sands. McKee (1966) put White Sands in the global spotlight as a model for the internal structure of eolian dunes. He made careful sketches based on bulldozed dune trenches. McKee and Douglas (1971) and McKee and Moiola (1975) later described aspects of the growth and sedimentology of the various dune types at White Sands, including the mysterious dome dunes. Fryberger and Dean (1979), Fryberger et al. (1983, 1984, 1988), Fryberger (2001a, 2001b), and Schenk and Fryberger (1988) described sedimentological aspects of the White Sands dune field and compared their observations with other (quartzose) dune fields. Kocurek et al. (2007) and Ewing and Kocurek (2010) studied the morphology of the dune field at White Sands, with some concepts from that work that applied to Mars. Mamer and Newton (2017) studied the Cuatrociénegas gypsum dune field in Coahuila, Mexico. That report sheds light on sedimentary processes there that are also common at White Sands. Interestingly, they include an excellent illustration of a shrub yardang on the cover of their report, and a dune yardang as their figure 22B. A recent paper by Holliday et al. (2023) identifies two significant dates for the origin and development of the White Sands dune field: an archeological site on a parabolic dune dates to 12,200 years ago, and a site in the barchanoid dune field is dated 8,770 years

ago during a period of Holocene regional aridity that continues today.

ANCIENT HUMAN TRACKWAYS

We mention the ancient human trackways studies because the erosion recorded by the yardangs at White Sands may shed light on the preservation and exposure of these features. The trackways were discovered in the early 2000s on the Alkali Flat, a region that has been deeply scoured by wind erosion during the Holocene. The scour-exposed ancient trackways may be the oldest known from North America (23–21 ka). These have been described in a series of landmark papers, including Bennett et al. (2019, 2020, 2021) and Bustos et al. (2018), who described human-sloth interactions. Urban et al. (2019) used 3D radar imaging to map trackways on the west side of the Alkali Flat. The discussion of the precise age and stratigraphy of the fossil footprints continues as new studies go forward (Rachal et al., 2021, 2024).

GEOMORPHOLOGY OF WHITE SANDS

Our study area at White Sands comprises the National Park and areas northward in the Tularosa Basin where yardangs occur along the paleoshorelines and erosional scarps in sediments of ancient Lake Otero (Fig. 7). Our study area thus extends roughly from Lake Lucero in the south to the Carrizozo Malpais basalt flows in the north.

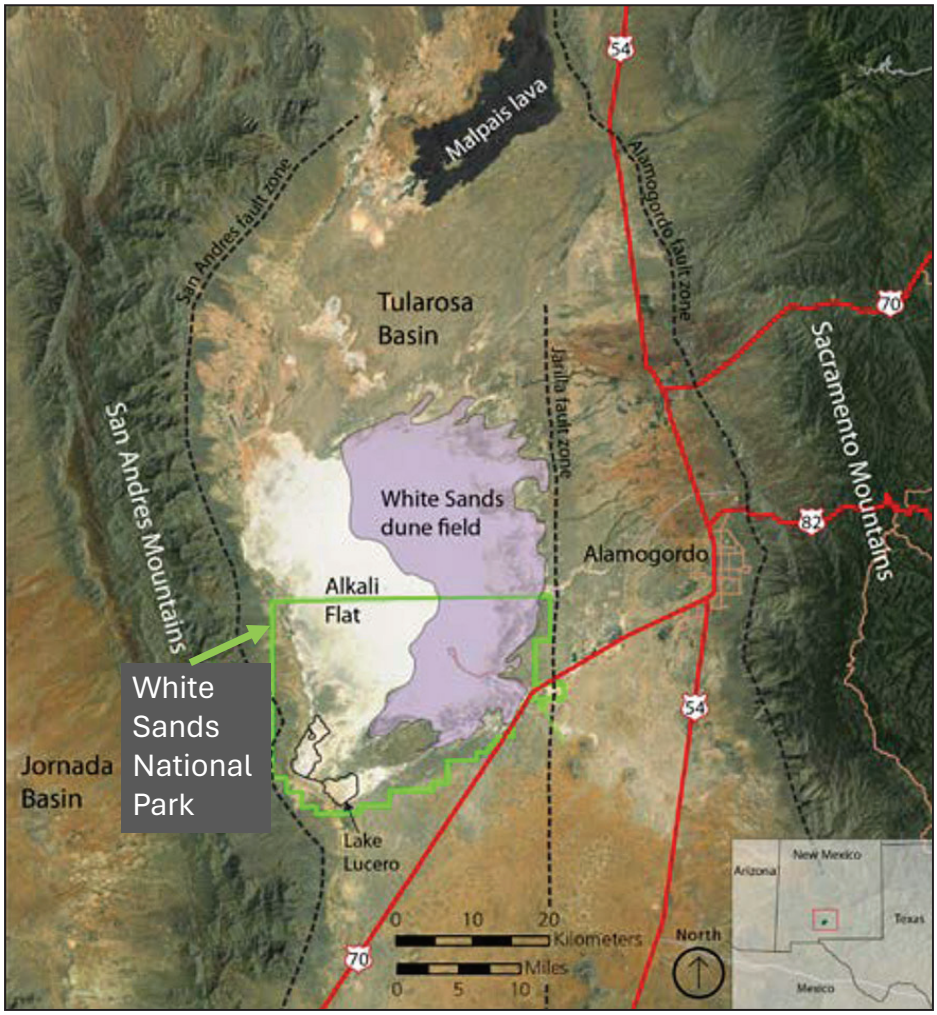

Figure 7. Overview map of the White Sands dune field and Alkali Flat in the Tularosa Basin, New Mexico. The outline of White Sands National Park is green and highways are red. The Tularosa Basin is bounded on the west by the San Andres Mountains and on the east by the Sacramento Mountains. After KellerLynn (2012) and Kocurek et al. (2007).

The geomorphology of White Sands is complex. It consists of several distinctive elements, including modern Lake Lucero, the Alkali Flat, and the scarps and shorelines composed mainly of ancient Lake Otero sediments. To the east of the old shorelines lie most of the parabolic and barchanoid dune fields of White Sands (Fig. 8).

The topographically low parts of the Alkali Flat comprise a Holocene (ephemeral) lake basin that includes Lake Lucero on the southwest side of the National Park (Fig. 8). The slightly higher scour platform (1–3 m higher relative to the lake/playa basin) lies to the east of the Holocene lake basin. Dune fields, deflationary terraces, and various yardangs (3–10 m higher) in turn border this area. The scarp yardangs are commonly formed from quartzose alluvium or the gypsiferous, shaly sediments of Lake Otero on the northern part of the Alkali Flat. On the west side of the Alkali Flat, the cliffs and deflationary terraces consist mainly of interbedded Lake Otero and alluvial sediments with few yardangs. Barchanoid and parabolic dune fields dominate the landscape immediately east of the Alkali Flat. All sediments become more quartzose from south to north at White Sands due to input from the various, mostly ephemeral drainages that empty into the Tularosa Basin, especially along the northern axis of the basin.

CLIMATE OF WHITE SANDS

Climatic parameters—especially wind and rainfall—are important to any study of yardangs. Wind direction and strength control much of the shape and orientation of yardangs. Precipitation and temperature impact the weathering processes of the lightly indurated gypsum sands that have been scoured by wind into yardangs at White Sands. For example, rainfall amount and timing affect the evolution of gullying along scarps where the interfluves have been scoured into yardangs.

The average annual rainfall at nearby Alamogordo is 330 mm (13 in.), most of which falls as thundershowers during the hot summer months from July through August (Fig. 9). In general, the White Sands climate falls roughly into the middle of the semiarid category for precipitation (250–500 mm of rain per year). Because of the heat and dry climate, evaporation rates are high (Figs. 10 and 11).

On the other hand, the peak season for wind energy release is during April and May, after the long dry spell following the summer rains of the previous year. Thus, most wind energy is expended at precisely the time of year when the land is driest due to lack of precipitation and high evaporation (Fig. 12). This seasonal offset of rainfall and wind energy may have contributed to the development of the yardangs at White Sands.

One quantitative way to assess wind energy is in terms of the potential for the wind to move sand (Fryberger and Dean, 1979). This method is basically a computation of relative potential sand movement by wind, called the drift potential (DP; Fryberger and Dean, 1979). Drift potential derives from the evaluation of an equation for wind energy using the percentage of a given time interval that the wind blows from a given direction multiplied by the wind velocity. The resulting calculation outcomes are referred to as "vector units" (VU) for simplicity because, however useful they may be, they are relative numbers that do not quantitatively predict sand movement.

The DP method also allows computation of the resultant effect of all winds (resultant drift potential, or RDP) and the resultant direction (RDD) of potential sand movement (Fryberger and Dean, 1979). This method allows easy comparison with other wind regimes around the world without having to make assumptions about grain size, rainfall, vegetation, or other factors that also influence sand movement by wind (Breed et al., 1979). The amount of sand moved by the wind, or eroded from yardangs by the wind, for example, also depends on variables of terrain and climate. Actual sand drift (AD) is best evaluated with sand-trapping devices to quantify the divergence of DP from AD.

At White Sands, the nearest weather station is at Holloman Air Force Base (AFB), located near the eastern margin of the White Sands dune field. The average monthly DP at Holloman AFB is at a maximum in spring (Fig. 13).

A more detailed analysis of DP, including wind direction, can be expressed as a "sand rose" diagram showing the potential sand drift from various directions upwind (Fryberger and Dean, 1979). A study of the bimonthly sand roses from Holloman AFB reveals the dominance of the winds from the

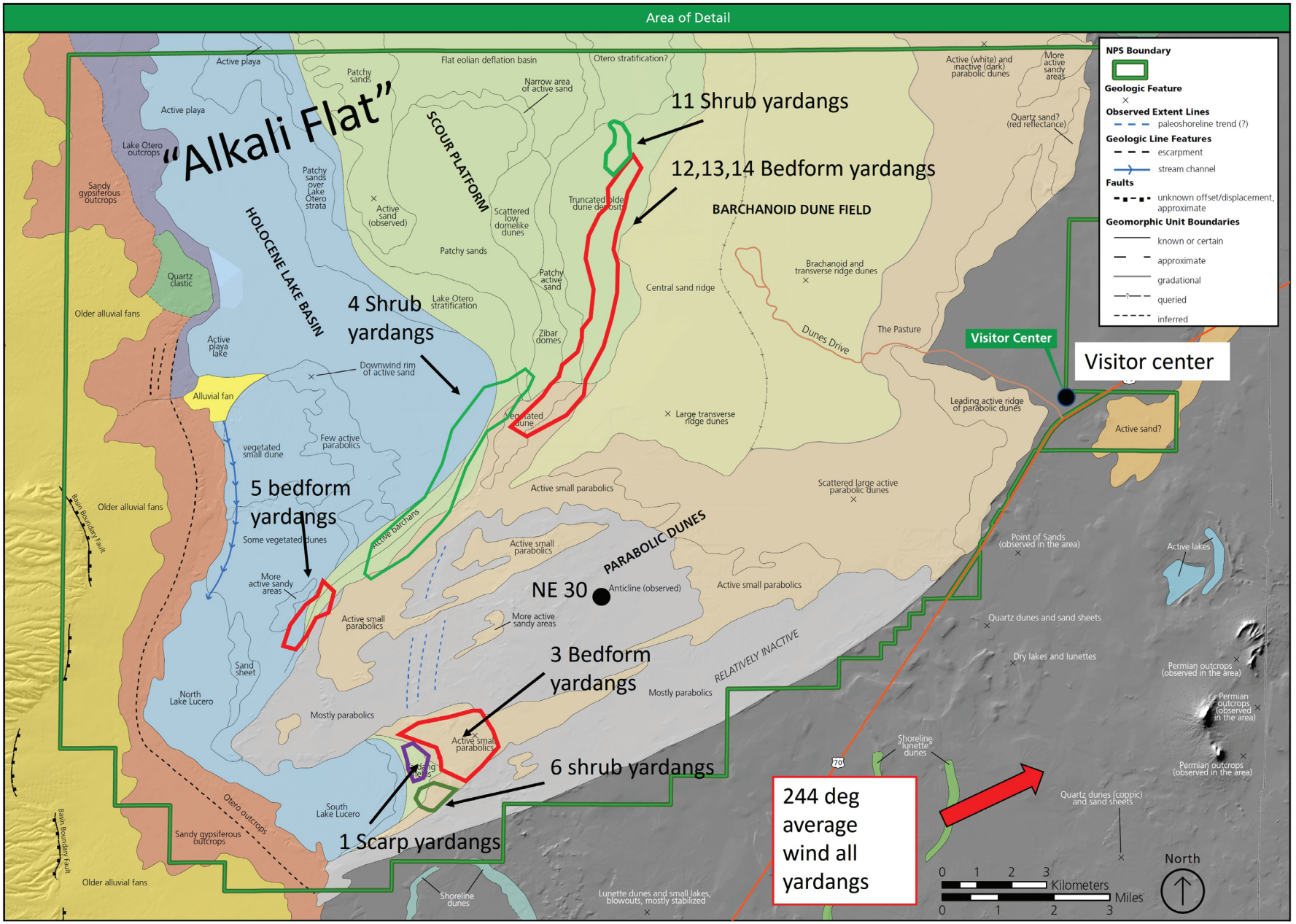

Figure 8. A geomorphic map of the surficial sediments within White Sands National Park. Our yardang study polygons that lie within the park boundary are outlined in red, purple, and green, reflecting the dominant yardang forms within. After original maps of Fryberger (2001a, 2001b) as published in KellerLynn (2012).

southwest. However, both annual and monthly sand roses also reveal significant potential sand movement from the northwest (mainly in winter) and the southeast (mainly in summer; Fig. 14). These multiple wind directions may have some impact on yardang development at White Sands. In sum, however, the yardangs throughout the Tularosa Basin align closely with the annual resultant drift direction (RDD). The annual drift potential (DP) of 149 VU noted in Figure 14, computed in 1979, indicates a low-energy wind environment (0–200 VU) compared to other desert regions (Fryberger and Dean, 1979).

We computed a new sand rose using a period of record that included all records to 2021 (Fig. 15). This resulted in a value of 323 VU, which would place White Sands at the higher end of the intermediate wind energy for deserts worldwide (200–400 VU; Fryberger and Dean, 1979, p. 150). The higher wind energy revealed by our present calculations may reflect stronger winds since 1979 or other factors such as location and type of recording equipment.

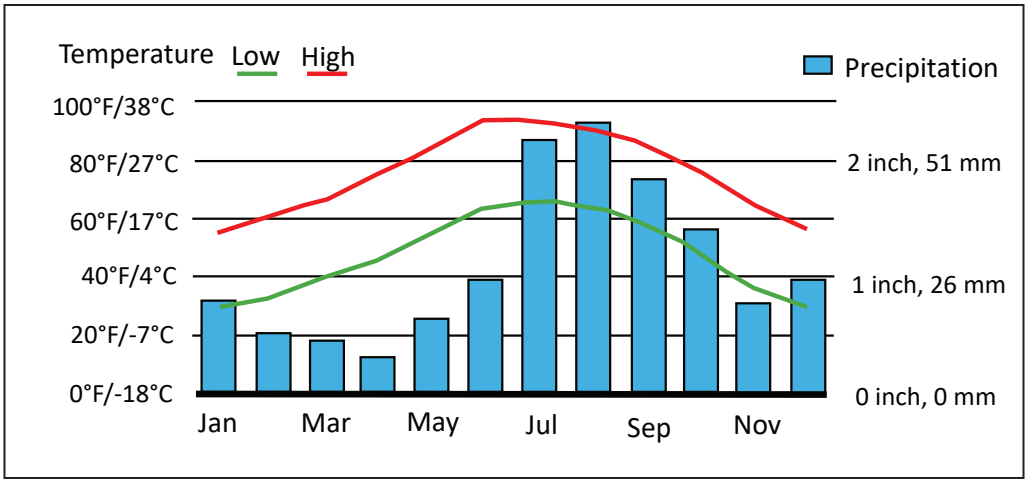

Figure 9. Chart of monthly average rainfall in inches and millimeters (mm) at Alamogordo, New Mexico. Annual precipitation at Alamogordo is roughly 13 inches (330 mm). Data source: U.S. Climate Data (2024).

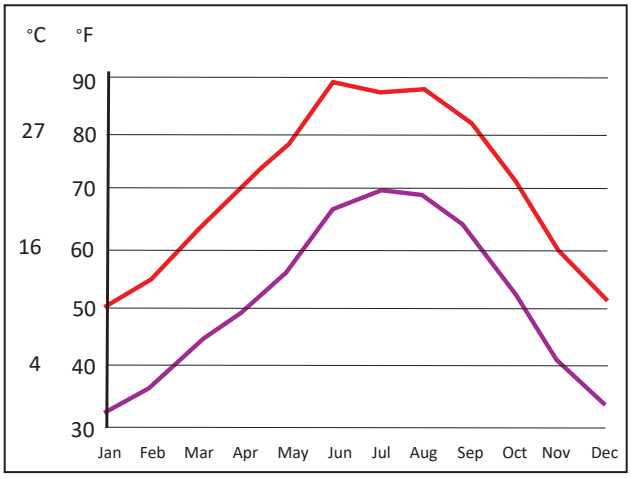

Figure 10. Average high (red line) and low (purple line) temperatures at Alamogordo, New Mexico during the year. Data source: Weather U.S. (2024).

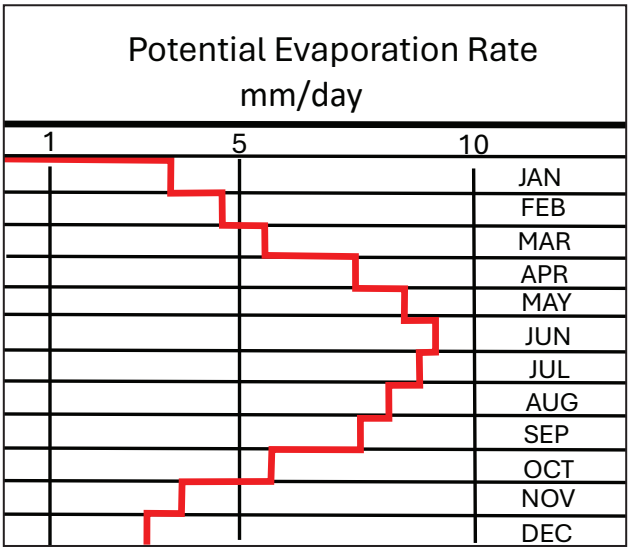

Figure 11. Evaporation rates during the year at White Sands. After Almendinger (1971).

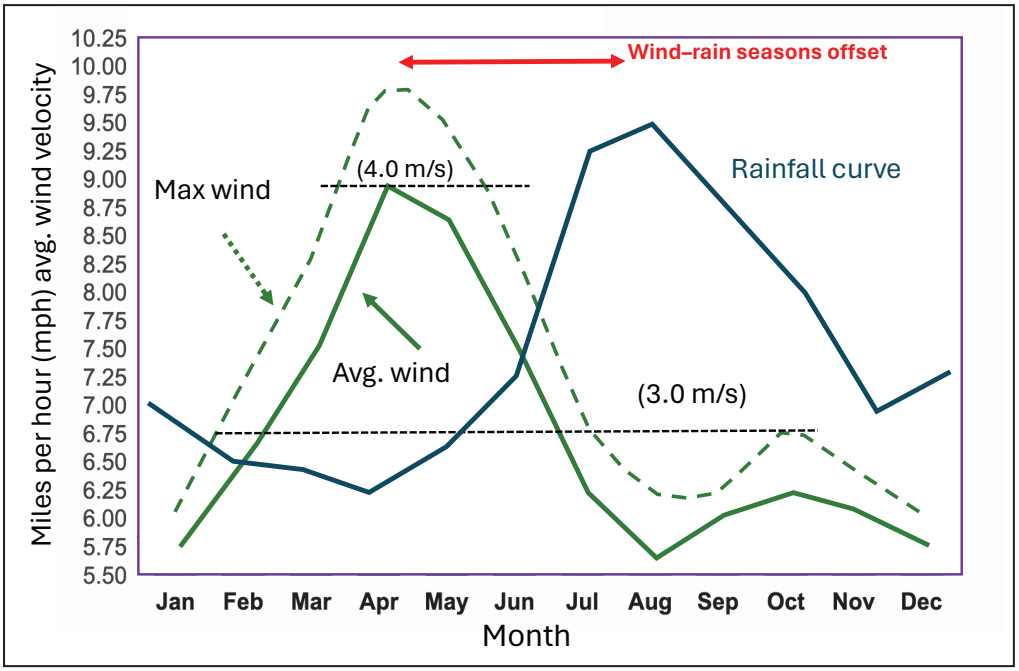

Figure 12. Average and maximum wind velocities by month, in miles per hour (mph; left axis) and meters per second (m/s; annotations) at Alamogordo, New Mexico, approximately 22 km ENE of the visitor center at White Sands. Also included is the rainfall curve from Figure 9 (no scale) placed on the graph to illustrate the offset of rainfall and wind seasons. This offset may have promoted the development of yardangs at White Sands. Data source: Weather U.S. (2024).

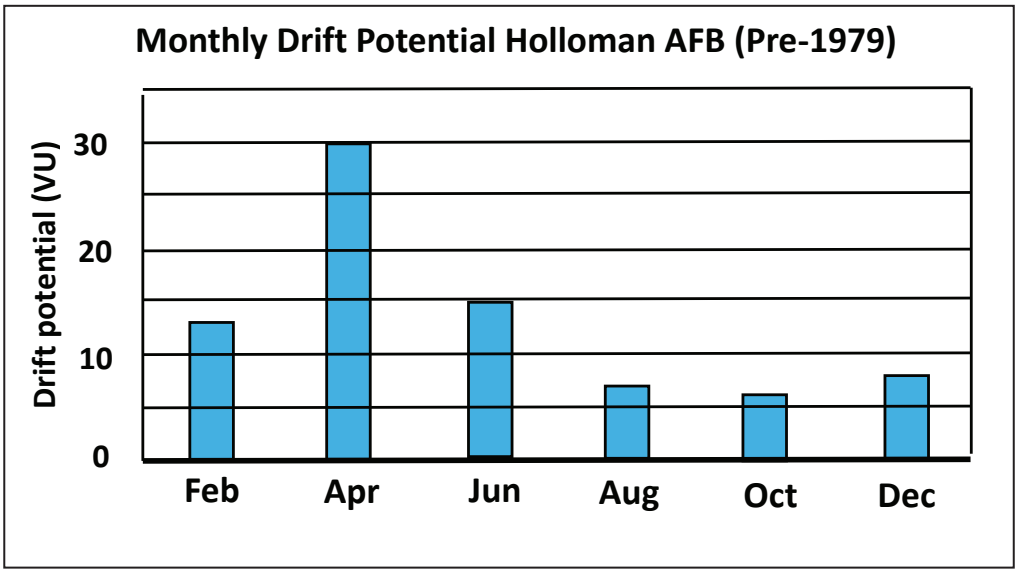

Figure 13. Bar graph showing drift potential during the year (bimonthly) at Holloman AFB. The spring peak in wind energy, mainly from the southwest, is caused in part by winds associated with cold fronts passing through in spring. This graph is based on records gathered by the National Climatic Center in Asheville, North Carolina.

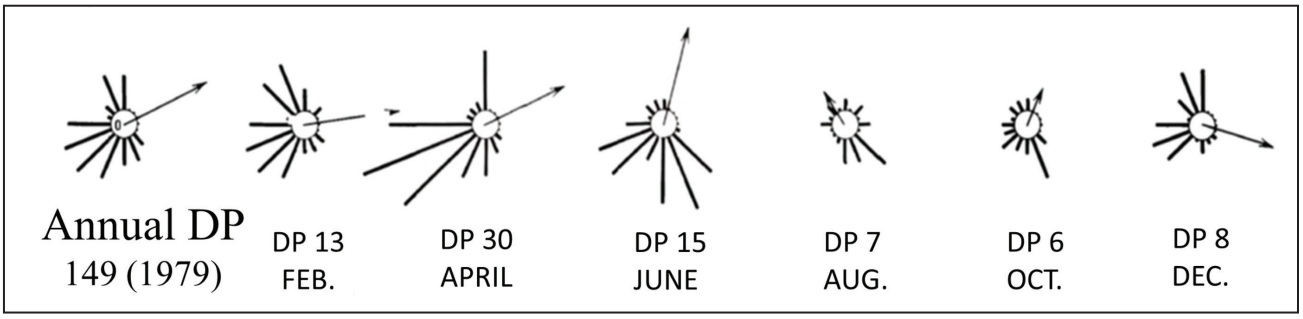

Figure 14. Annual and monthly sand roses for Holloman AFB on the east side of the White Sands dune field, roughly 10 km northeast of the White Sands National Park visitor center.

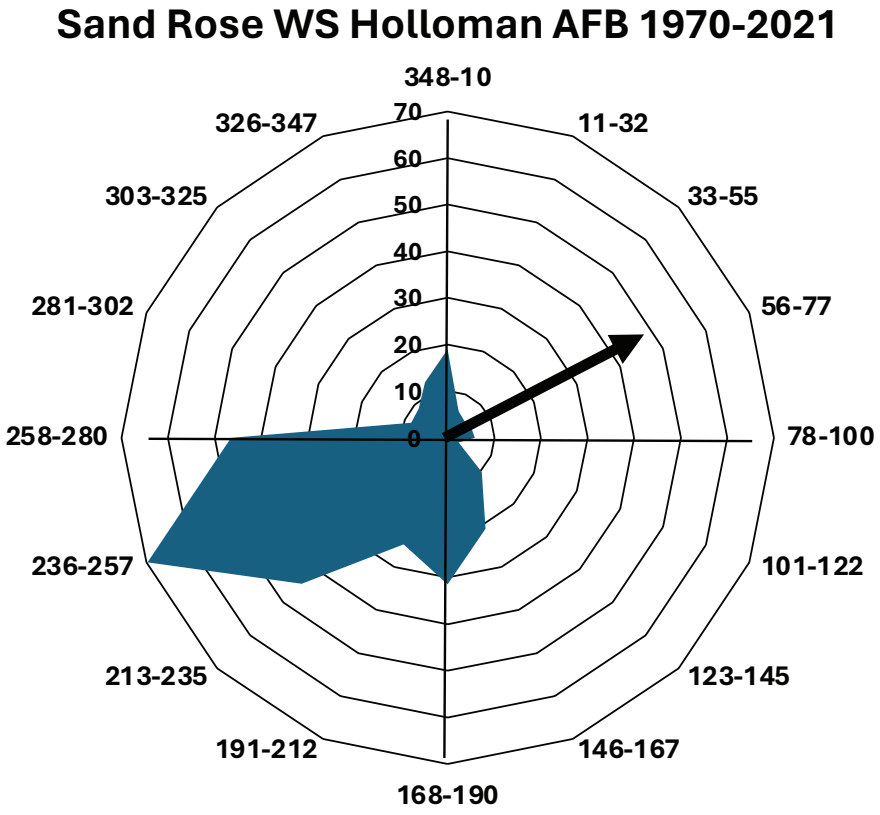

Figure 15. A new (2021) annual sand rose for Holloman AFB (near White Sands) calculated for this study. This rose incorporates more-recent data than our earlier roses shown in Figure 14. Blue shading represents the sand-moving potential of winds from the associated direction. Although the wind energy (drift potential [343 VU]) is higher, the basic modes of the wind direction are similar. Data were from the Iowa State University Environmental Mesonet (2024).

METHODS OF STUDY

An important aspect of our study was the analysis of photographs and notes we took during our fieldwork to describe, classify, and illustrate different kinds of yardangs at White Sands. We were interested in knowing the geographic distribution of the scarp, bedform, and shrub yardangs at White Sands and learning more about how they formed.

We also measured the distribution and dimensions of the scarp, bedform, and shrub yardangs using aerial photographs and Google Earth satellite views. Polygons drawn on our satellite views enclosed many of the numerous good examples of yardang types visible on the Google Earth imagery. We measured yardangs within the selected polygons and summarized our measurements in graphical form. We made note of the heights of yardangs where possible; however, the elevation data from the satellite imagery we had were not accurate enough to measure heights on smaller yardangs.

Commonly, either scarp, bedform, or shrub yardangs were the dominant type in particular settings. The excellent resolution of Google Earth imagery at White Sands allowed us to record reasonably accurate measurements of length and width for each type, down to about 1 m.

RESULTS OF THIS STUDY

OVERVIEW OF STUDY AREAS AND YARDANG TYPES AT WHITE SANDS

Scarp yardangs are the largest we observed, both in terms of height (several meters) and length (20 m or more), and thus were relatively easy to find and measure in satellite imagery (Table 1). They are typically found at breaks in slope along late Pleistocene and Holocene lake shorelines where sediments are indurated enough to resist wind erosion. The best examples are in study area 1 (east of Lake Lucero) and study areas 2 and 15 in the north, roughly along the L1 shoreline of Langford (2003) that formed during the Pleistocene–Holocene transition (Fig. 16). In the north, a sharp break in slope lies between the scour platform and cliffs to the east.

We summarize in Table 1 the average parameters for each of the study areas (polygons created in Google Earth) at White Sands (Fig. 16). We did not find enough large yardangs in study area 18, along the west side of Lake Lucero, to make measurements of yardangs. Our informal look at the streamlined islands (which we are not sure are true yardangs, per se, because they may be constructive features) along the west side of Lake Lucero and the Alkali Flat yielded ratios of width to length of approximately 0.56, like the higher ratios observed for bedform yardangs.

The scour platform of the Alkali Flat (see Fig. 8) is only a meter or two higher than the Holocene lake basin to the west. However, the platform is also several meters lower than the shorelines and retreating scarps of the Lake Otero sediments that surround it. Our original intent in using the term "scour platform," as shown in Figure 8, was to define the area of most frequent exposure to wind erosion, as opposed to the Holocene lake "basin" along the west side of the Alkali Flat that floods more frequently due to precipitation runoff (Fryberger and Ormerod, 2023). Wind erosion nevertheless does occur in the Holocene lake basin when it is dry. The boundary between the Holocene lake basin and the scour platform roughly follows the 1,191.5 m above mean sea level contour (Figs. 8 and 16).

We found that many of the bedform and shrub yardangs at White Sands are distributed along or between the L2 and L1 shorelines proposed by Langford (2003) and below the ultimate high shoreline identified by Allen et al. (2009) at 1,204 m using geological evidence (Fig. 16).

The yardang concentrations we mapped also closely follow the trend of eroding Lake Otero sediments where there are no obvious shoreline sediment buildups, for example, lunette dunes or barriers such as those at Lake Estancia 190 km to the north (Allen and Anderson, 2000; Allen, 2005).

ORIENTATION OF YARDANGS AND WIND REGIME

As described in the climate review above, the present-day wind regime at White Sands is of low to moderate energy, with a dominant wind direction from the southwest (Figs. 13–15). Although there are two other significant subsidiary modes of the wind regime, it appears that the southwest mode has determined the alignment of virtually all the yardangs we studied (Fig. 17).

The effects of subsidiary modal wind directions from the north and southwest (as shown in Figs. 14 and 15) may be the ultimate cause of the slight difference in alignment between the RDD and the yardang alignments, although how this process might work is a matter for further study.

Table 1. Summary of the measurements of yardangs in this study. See Figure 16 for locations of the study polygons.

Polygon	Dominant Yardang Type	Description	Average Upwind Direction (degrees)	Proximal Shoreline (after Langford, 2003)	Average Length (m)	Average Width (m)	Comment
1	Scarp	Large yardangs evolved from playa sediments, east shore of Lake Lucero	250		23.2	6.2	Probably Lake Otero sediments
2	Scarp	Large yardangs evolved from earlier gullies in cliff, north area	241	L1	20.0	5.2	Probably Lake Otero sediments
3	Bedform	Mostly in eroded parabolic dunes east of Lake Lucero	241	L2	11.3	4.2	Mostly bare (vegetation-free) yardangs, with a few shrub yardangs
4	Shrub	Shrub yardangs along shoreline north of Lake Lucero	241	Between L1-L2	16.7	10.5	Mostly round shapes centered on saltcedar bushes, commonly with smooth sides
5	Shrub	Shrub yardangs in parabolic dunes east of shoreline of north lobe of Lake Lucero	246	Lake Lucero	19.1	8.5	Shrub yardangs, a few bedform (dune) yardangs
6	Shrub	Shrub yardangs on southeast shore of Lake Lucero, just south of polygon 1	248	Lake Lucero	15.7	9.3	Numerous small (less than 10 m length) bedform yardangs in parabolic interdunes
7,8	Shrub	Near west margin of dune field	234	L1	23.8	12.2	Mix of shrub, playa, or interdune?
9,10	Bedform	Near west margin of dune field and east margin of scour platform	231	Between L1-L2	8.1	4.4	
11	Shrub	Near west margin of dune field and east margin of scour platform	239	Between L1-L2	18.6	11.2	
12,13,14	Bedform	Within west area of main dunes (dune ridge)	243	Between L1-L2	9.8	4.8	Many small yardangs scoured from cohesive dune sand; some follow dune bedding if aligned with wind
15	Scarp	North area along old shoreline	236	Between L1-L2	12	5.9	Yardangs in part evolved from fluvial channels in escarpment
16	Shrub	West (upwind) side of dunes	248	Straddles L1	18.1	16.3	Rounder shape than purely aerodynamic yardangs due to saltcedar
17	Bedform	In west part of main dune field	243	No obvious shoreline	6.6	4.4	Mostly small bedform (dune) yardangs in early cemented sands, some are relict from saltcedar shrubs
18	Scarp	Along west side of Lake Lucero	239	L1-L2	Small	Small	Streamlined islands with scattered small yardangs, especially on upwind side

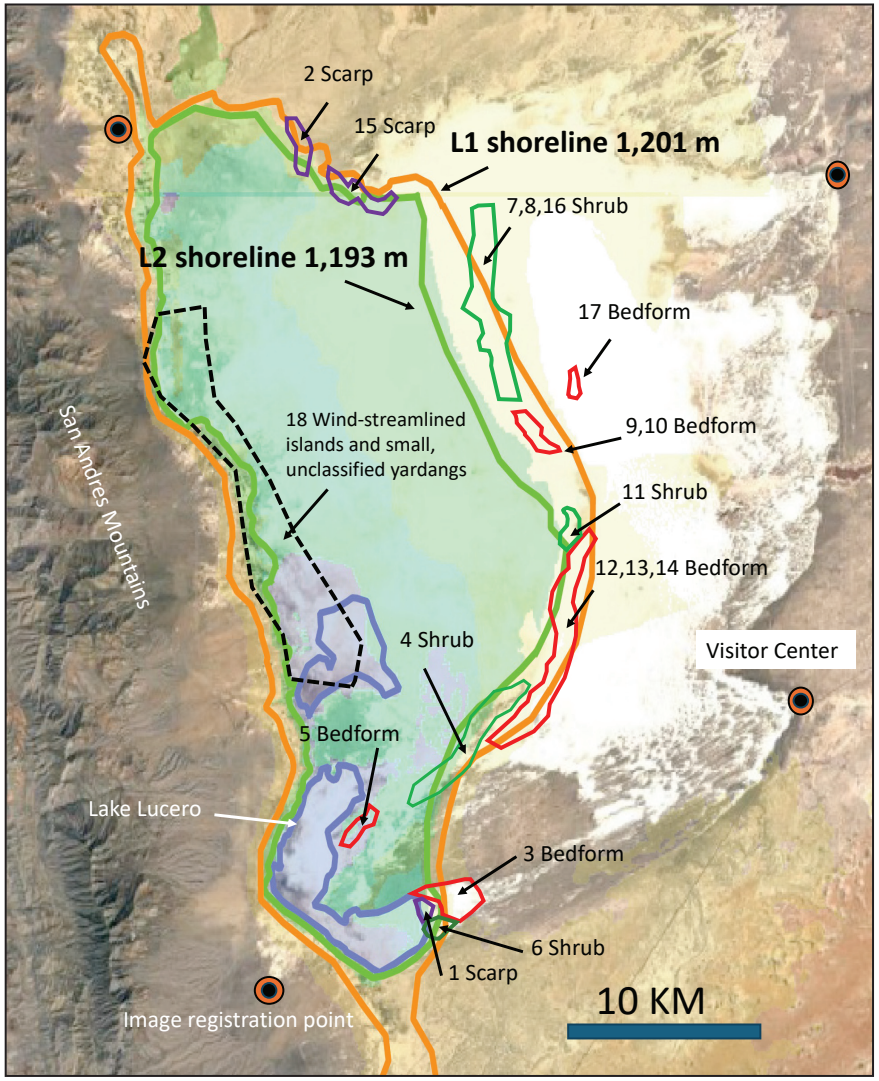

Figure 16. Yardang study areas (polygons) superimposed on a satellite image of White Sands. There is a clear association of yardangs with the shorelines of Lakes Otero and Lucero. The green and orange lines follow the L2 and L1 shorelines (formed during the Pleistocene–Holocene transition), respectively, of ancient Lake Otero proposed by Langford (2003). Major Holocene shorelines, including Lake Lucero, are outlined in blue. Lake Otero shorelines lie at approximately the elevations marked with labelled arrows. Allen et al. (2009) place the Lake Otero highstand shoreline at approximately 1,204 m, 3 m higher than Langford (2003) at 1,201 m. Colored polygons encompass areas dominated by a particular type of yardang. Scarp yardang polygons are purple, bedform yardang polygons are red, and shrub yardang polygons are green. Arrows with numbers designate the areas (polygons) of this report in which measurements of yardang length and width were made. After Langford (2003) and Allen et al. (2009).

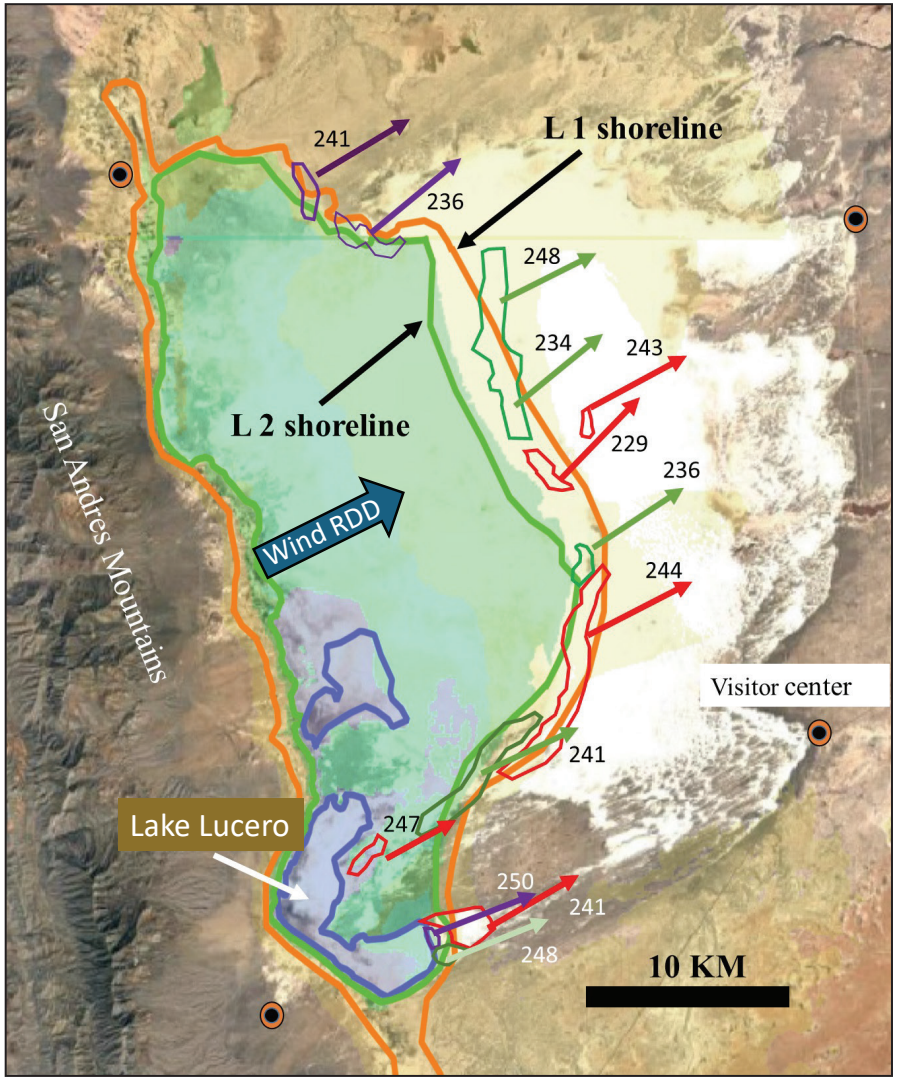

Figure 17. The effective wind directions (in degrees) recorded by the yardangs we studied at White Sands National Park, shown by colored arrows. Our study area polygons are outlined here on the Langford (2003) shoreline map and a satellite image background. Colors of outlines show dominant yardang types within each polygon: purple = scarp yardangs, red = bedform yardangs, and green = shrub yardangs. Regardless of type, most yardangs are aligned closely with the resultant drift direction (RDD) of the wind regime at White Sands, as represented by data from nearby Holloman AFB.

GEOMORPHOLOGY OF SCARP YARDANGS

Scarp Yardangs in Study Area 1, Eastern Shore of Lake Lucero

At White Sands, scarp yardangs are mostly sculpted from playa sediments that were deposited by drying Lake Otero and possibly sediments of younger Lake Lucero (Figs. 18 and 19). These sediments are generally gypsiferous and flat-lying, or wavy due to haloturbation or bioturbation. In a few places, the bioturbation is by Pleistocene mammoths, ground sloths, and early humans (Bustos et al., 2018; Bennett et al., 2020).

The scarp yardangs at study area 1 (Fig. 16) east of Lake Lucero have the classic rounded prow upwind with a tapering stern. However, the top of the yardang (or "keel") can be quite irregular in plain view, forming a flat surface atop the yardang due to resistance to wind erosion of the caprock of coarse gypsum grains.

At study area 1 (Fig. 16) along the eastern shore of Lake Lucero, the yardangs have evolved from interfluves between ephemeral drainages that drain onto the playa. Figure 20 illustrates schematically how these yardangs evolved at White Sands. Runoff from higher ground onto the Alkali Flat first creates gullies. The interfluves are gradually streamlined to form yardangs (shaded yellow in Fig. 20) facing into the dominant southwest wind. Wind erosion also smooths and rounds the floors of the gullies.

In settings such as this, near a possible abandoned shoreline (Langford, 2003), the depth to which wind presently scours appears to be set by the level of the groundwater table on the Alkali Flat rather than by remnants of an actual lake. This is because the damp sands and precipitated evaporites near the water table resist wind erosion. The long-term tendency at White Sands has been for abandoned shorelines to be preserved as a series of subtle terraces or lunettes as Lake Otero dried. This process was intermittent, comprising episodes of rise and fall of the lake level with the ultimate complete drying of Lake Otero (Allen et al., 2009).

During the Holocene, various terraces along abandoned shorelines were wind-scoured, creating yardangs even as the Alkali Flat was scoured deeper (Langford, 2003; Allen et al., 2009; Baitis et al., 2014). This process is like that described by Szynkiewicz et al. (2010), as shown in their figure 8.

It is common for yardangs at the Lake Lucero (study area 1) locality to have a two-part vertical profile, with a steep upper part and a gently sloping lower part, as shown by the red dashed line in Figure 21.

Scarp Yardangs in Study Areas 2 and 15, Northern White Sands

Our study areas 2 and 15 (outlined in purple in Figs. 16 and 17) have scarp yardangs that are the largest—and most aerodynamically mature—of all that were observed in the study. They align with the dominant southwest wind regime. In some places, they are "half yardangs" in the sense that many of them merge smoothly downwind into the higher terrain from which they have been sculpted by wind (Fig. 22). Most of the yardangs are gullied along the sides, with a smooth, rounded prow on the front. The prows tend to be stepped, the result of differential erosion of horizontal layers within the sediment. Some are tapered to a smooth keel and thus exist as a standalone yardang; others have a well-developed prow that merges into higher ground to the northeast (Fig. 22).

In study areas 2 and 15, there are places where there are several sets of yardangs (for a view of yardangs in study area 15, see Fig. 5A). The largest are well-formed and eroded from dark sediments of Lake Otero that make up the higher ground. This higher ground is roughly at an elevation of 1,200 m, which is close to the 1,204 m highstand for Lake Otero documented by Allen et al. (2009). Smaller yardangs exist on subtle terraces at lower elevations upwind.

Yardangs such as these, formed from poorly indurated sediment, may or may not be preserved in the geological record. There are yardangs in other places in the world, for example, Egypt, that have been cut into well-consolidated sediments. These features naturally have a higher probability for preservation in the geological record, especially in places where they might be buried, for example, by migrating eolian dunes (Tewes and Loope, 1992).

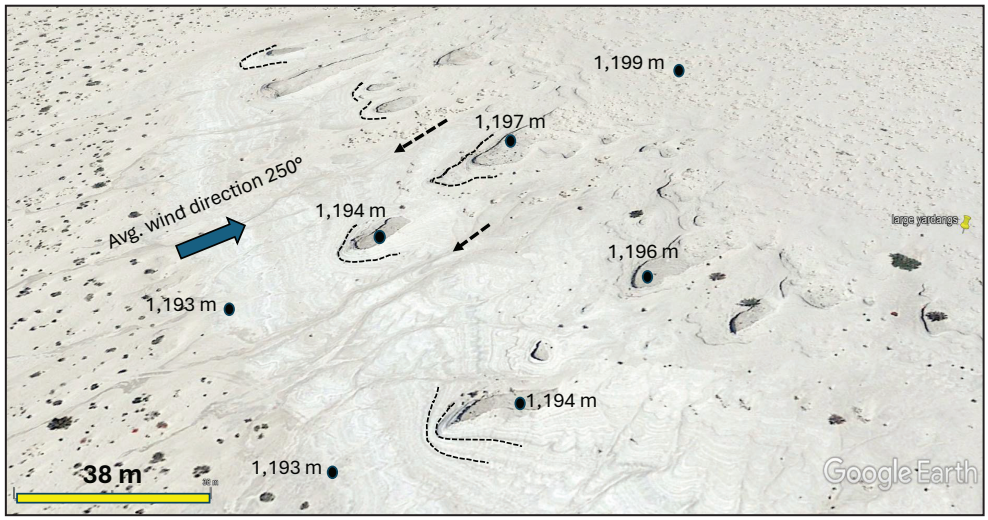

Figure 18. A satellite image showing scarp yardangs in study area 1. They have been carved from flat-bedded sediments of ancient Lake Otero. They consist mainly of gypsum crystals. These yardangs evolved from the interfluves between the ephemeral drainages. Dashed arrows show two of the drainages. Black dots are spot elevations. These yardangs are on a gentle rise in slope between the L1 and L2 shorelines of Langford (2003). Although the tops of the yardangs are irregular, flattish surfaces, the lower parts of the yardangs have been streamlined by wind erosion, as indicated by dashed lines following topography upwind of selected yardangs. Vertical exaggeration is 3×. Spot elevations and satellite image courtesy of Google Earth.

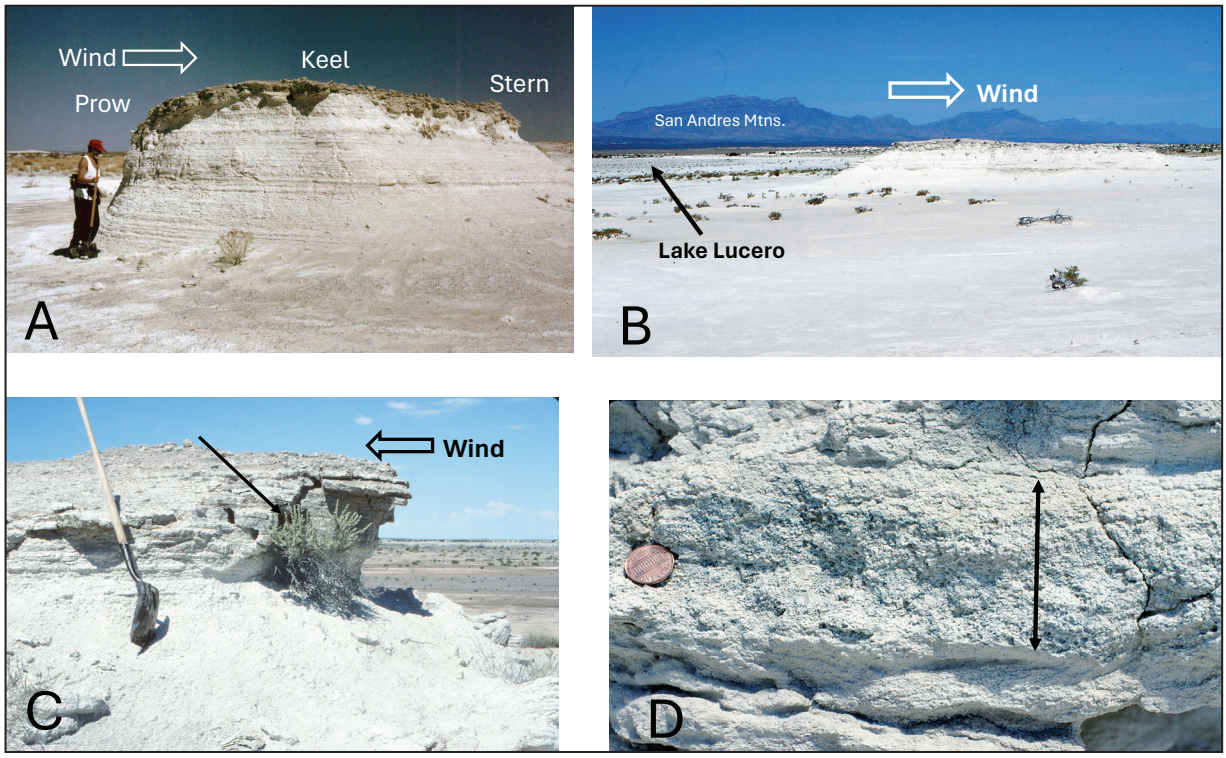

Figure 19. Scarp yardangs along the eastern margin of Lake Lucero. (A) The flat bedding within this yardang is the product of an evaporative phase of ancient Lake Otero. This yardang resists erosion due to a caprock of cemented coarse sand. Cements are mainly gypsum and calcite. (B) View to the northwest, showing a yardang aligned with the southwest winds, not far from the present shoreline of modern Lake Lucero that lies to the left in this image. (C) The prow of a scarp yardang near Lake Lucero. The yardang has flat and irregular bedding, capped by a resistant layer of cemented sand. Wind erosion is gradually undercutting the top of the yardang prow, which appears ready to collapse—a vertical crack is shown by a black arrow. The view is toward the southeast. Similar features have been described at Rogers Dry Lake, California, by Blackwelder (1934) and Ward and Greeley (1984). Shovel for scale. (D) A close view of a thin layer of coarse gypsum crystals (shown by arrow) within a yardang. A U.S. penny on the left provides scale. Crystals such as these were deposited on the floor of the Lake Otero when it had become a playa during the Holocene (Allen et al., 2009).

The wind-formed nature of the yardang fields at White Sands can be recognized, in part, by the near-perfect conformance of individual yardang orientations with each other and with the regional southwest wind. Contiguous outcrop areas not facing the wind have not developed yardangs (Fig. 23).

It is possible that, in addition to the abrasive power of sand mobilized from the Alkali Flat, the acceleration of wind over the rising ground downwind of the deflation basin (Alkali Flat) also promotes the formation of yardangs. This process may also have occurred on Mars, where yardangs often face into a wind that flows up scarps with over a thousand meters of relief. Examples may be found in the Martian mid-latitudes (Medusae Fossae Formation) using the Google Mars website. For published examples, see Ward et al. (1985) and Zimbelman and Griffin (2010).

Most of the yardangs at White Sands are not conspicuously elongate compared to some other regions of the world (McCauley et al., 1977a, 1977b; Whitney, 1985; Goudie, 2007, 2008; de Silva et al., 2010; Sebe et al., 2011; Hu et al., 2017). This is probably due to weak induration of the sediments at White Sands, which facilitates rapid erosion and retreat of the yardangs downwind as the scarp erodes (Fig. 24).

GEOMORPHOLOGY OF BEDFORM YARDANGS

Bedform yardangs at White Sands are commonly carved from partly cemented dunes. Unlike most scarp yardangs at White Sands, bedform yardangs are not a product of an interaction of fluvial and eolian processes. Moreover, since they are most common in the dry, slightly elevated terrains of the dune fields, they are less impacted by subregional deflation to the water table, as is the case with scarp yardangs.

Some bedform yardangs occur as isolated, relict features upwind of the dune from which they were formed because the dune has migrated downwind (Fig. 25). In such instances, the dune rebuilds its shape as it advances, replacing the sand left behind

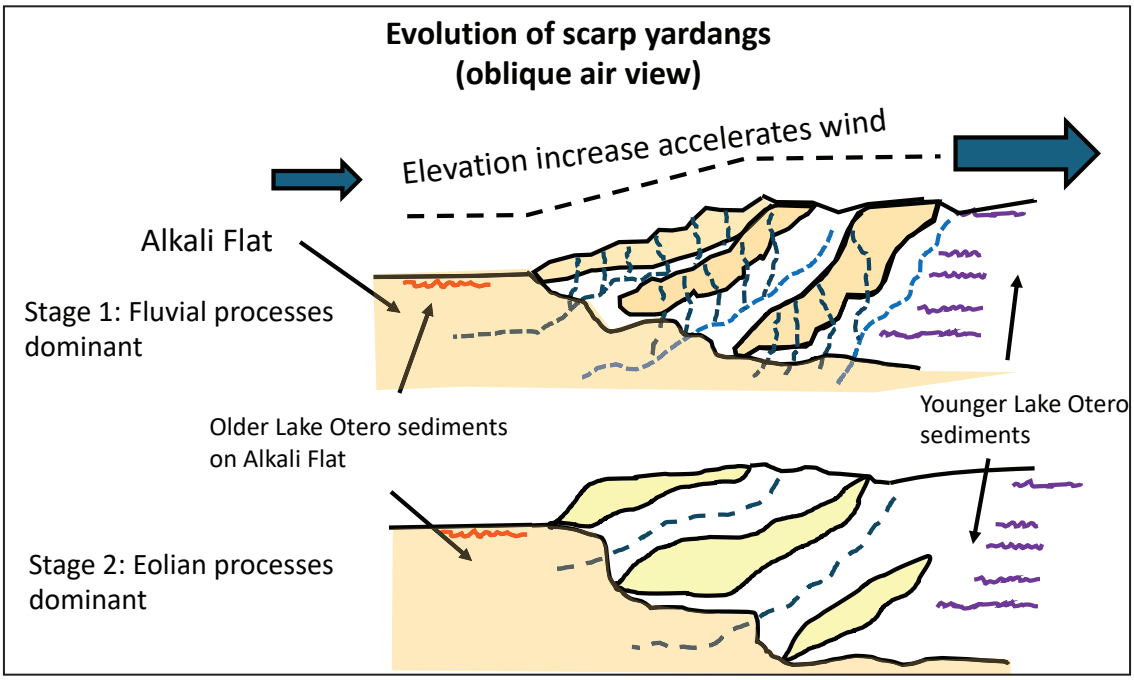

Figure 20. Formation of scarp yardangs. At White Sands, many yardangs (shaded light yellow in the lower panel) have formed at the transition between the wind-eroded Alkali Flat and elevated areas of uneroded sediments to the east. Cementation associated with abandoned shorelines, as well as case hardening of exposed gypsiferous sediment, left elevated areas that resisted scouring long after Lake Otero had disappeared. Scarp yardangs at White Sands only develop where interfluves face into the southwest wind. Crosswind areas are dominated by fluvial geomorphology, with little evidence of yardang formation. Red and purple wiggly lines symbolize bedding of older and younger Lake Otero sediments, respectively. Blue dashed lines show paths of drainages.

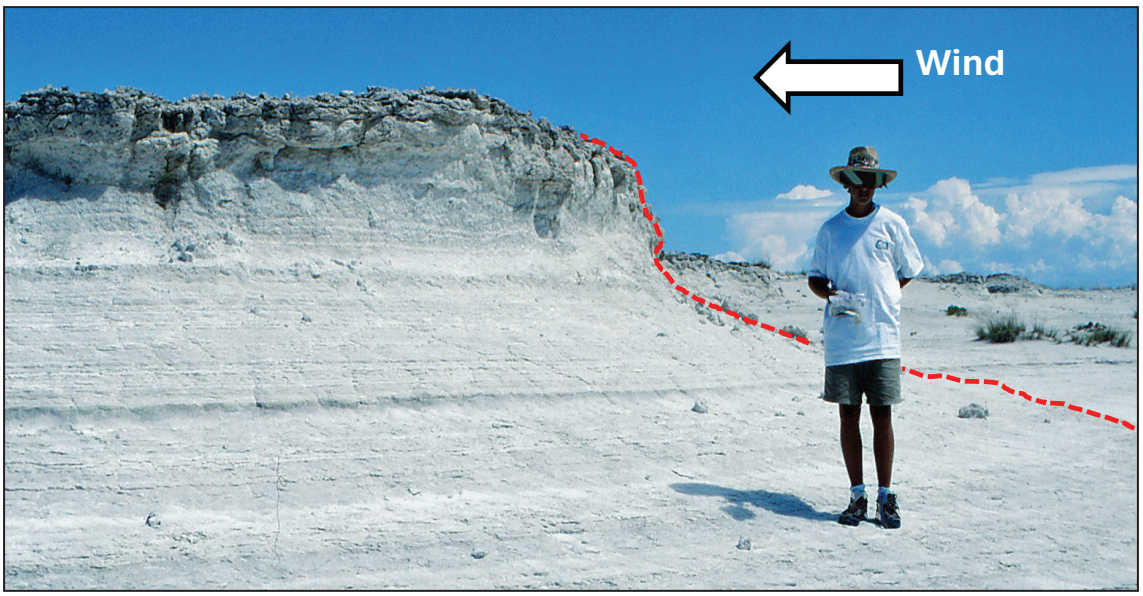

Figure 21. The prow of a yardang in study area 1, immediately east of Lake Lucero, showing flat, gypsiferous playa bedding with a steep slope near the top of yardang (shown by dashed red line). A coarse cemented layer on the top of the yardang has resisted wind erosion and thus created the flat upper surface typical of yardangs at this locality.

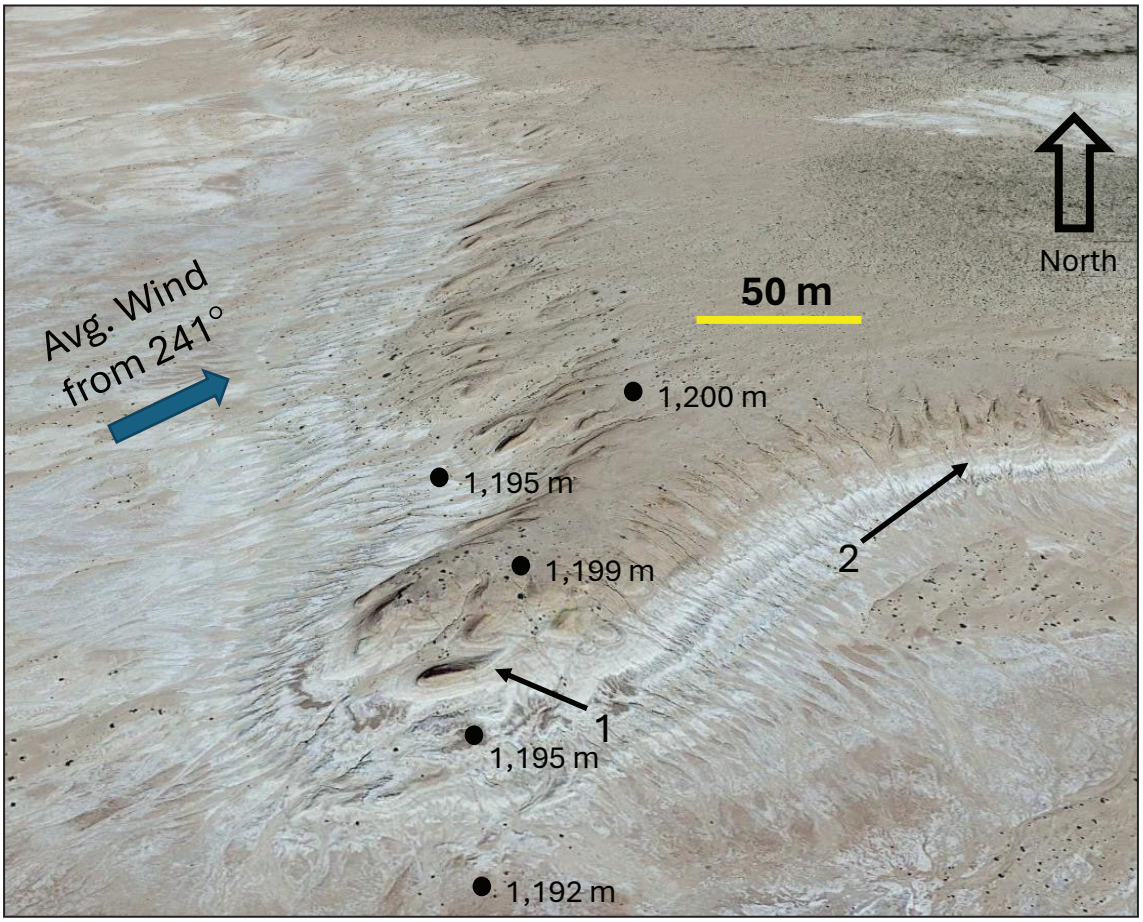

Figure 22. Satellite view of the southern part of study area 2. This area is located at the northeast margin of the White Sands dune field (see Figs. 16 and 17 for precise location). Winds blowing from the southwest have smoothed the interfluves, creating relatively mature scarp yardangs. We highlight one yardang (black arrow 1) that is topographically distinct from the higher ground to the northeast. Yardangs are absent where gullies do not align with the dominant southwest wind (black arrow 2). This image and elevations are courtesy of Google Earth. Vertical exaggeration is 3× in this view.

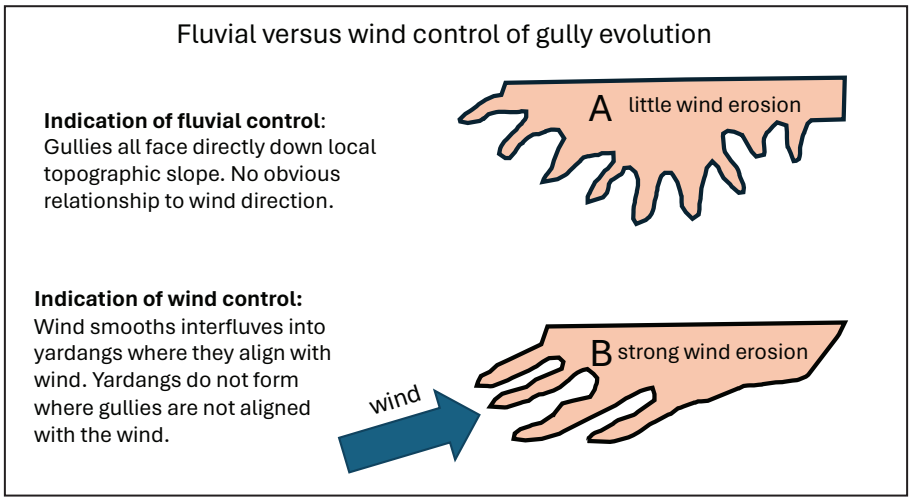

Figure 23. Sketch illustrating contrasting morphologies of drainage networks and yardangs with and without wind control of evolution. (A) In settings where only slope controls the evolution of fluvial channels and interfluves, all gullies tend to extend directly downslope. (B) In settings such as White Sands, where a dominant wind from a single direction has interacted with the fluvial system, yardangs form from those interfluves that extend roughly parallel to the prevailing wind. At White Sands, interfluves where drainage is perpendicular to the prevailing southwest winds seldom develop into yardangs, perhaps because of sheltering from the dominant wind.

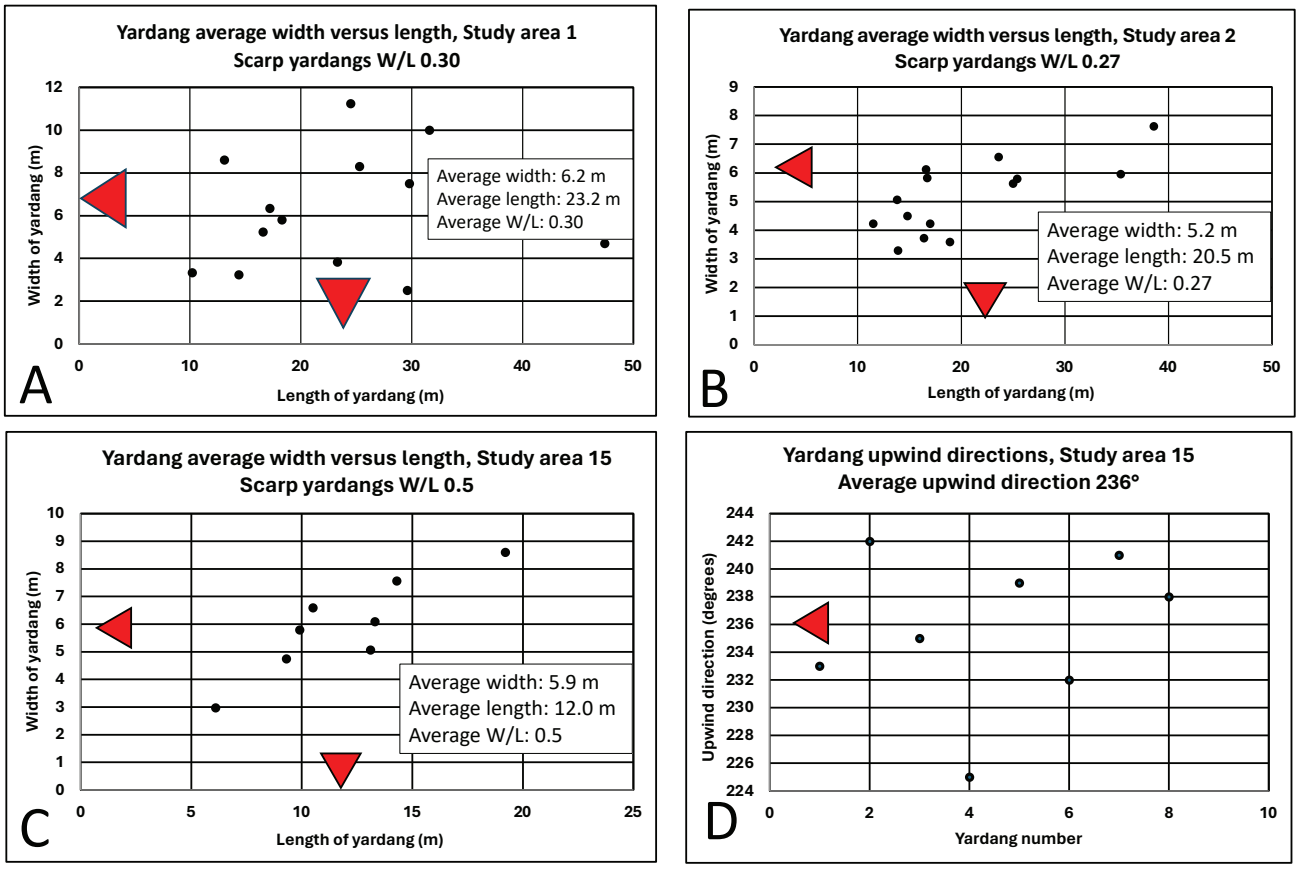

Figure 24. Yardang width versus length in study areas 1, 2, and 15 that are dominated by scarp yardangs, and effective formative wind direction. Red arrows indicate averages. (A) Study area 1, along the eastern shoreline of Lake Lucero. There is a wide spread of shapes implied by the data. (B) Study area 2 data. (C) Study area 15 data. The tighter distributions in study areas 2 and 15, which are reflective of more consistent shapes, imply greater aerodynamic maturity than the scarp yardangs in study area 1. (D) The average upwind direction measured on scarp yardangs in study area 15, which is representative of most of the scarp yardangs at White Sands (see also Figs. 17 and 36D).

as part of the yardang. At White Sands, bedform yardangs form because parts of the dune may be partially cemented by gypsum dissolved by meteoric water and later precipitated within the dune by drying. In some areas, early cementation by calcite occurs due to settling of airborne calcareous dust or incipient soil formation. The cemented primary strata can consist of cross-bedded eolian avalanche, grainfall, or ripple strata, or they might consist of irregular eolian interdune strata formed by grainfall and ripple deposition in association with salt ridges (Fryberger et al., 1983).

For this study, we use the term "bedform" yardang in a broad sense to encompass dune, interdune, sand sheet, and sabkha sediments and the many kinds of sedimentary structures among them (McKee, 1966; McKee and Douglass, 1971; McKee and Moiola, 1975; Fryberger et al., 1983, 1984). Zones of cementation in this environment are often fabric-selective, with texture as the main control, as described by Schenk and Fryberger (1988) and Schenk (1990). Eolian ripple strata are commonly better cemented than avalanche strata due to tighter packing and heterogeneous micro-permeability related to the pinstripe laminations formed between individual ripples. The complexity of fabric-selective cementation results in a wide variety of shapes and sizes of yardangs—including micro-yardangs a few centimeters in length on the floor of some interdunes. Nevertheless, many bedform yardangs are up to 10 m in length and several meters high (Fig. 26). The largest yardangs are impressive when encountered in the field and often have well-streamlined shapes close to the ideal 0.25 width-to-length ratio for lowest wind resistance by aerodynamic forms (Ward and Greeley, 1984). Bedform yardangs at White Sands are limited in size to the cemented portions of the dune or other eolian facies from which they formed (Fig. 27).

Patterns of early fabric-selective cementation may cause misalignment of a yardang relative to the wind or create a row of yardangs arranged in a crosswind trend (Fig. 28). This can occur because cemented eolian primary strata that are close to the wind, but not aligned perfectly, may form yardang shapes that align somewhere between the direction of the dominant southwest wind and the alignment of the cross-bedding. This phenomenon has also been described by Pelletier et al. (2018, see their figure 3) in bedrock at Ocotillo Wells, California, USA. If cemented layers are oblique to the wind, they are commonly eroded as a string of yardangs along the trend of cementation, with each yardang aligned to the wind, as shown in Figure 28. In addition, wind may be deflected locally around dune topography during the formation of a yardang on the windward slope, creating a slight misalignment of an individual yardang with the regional wind.

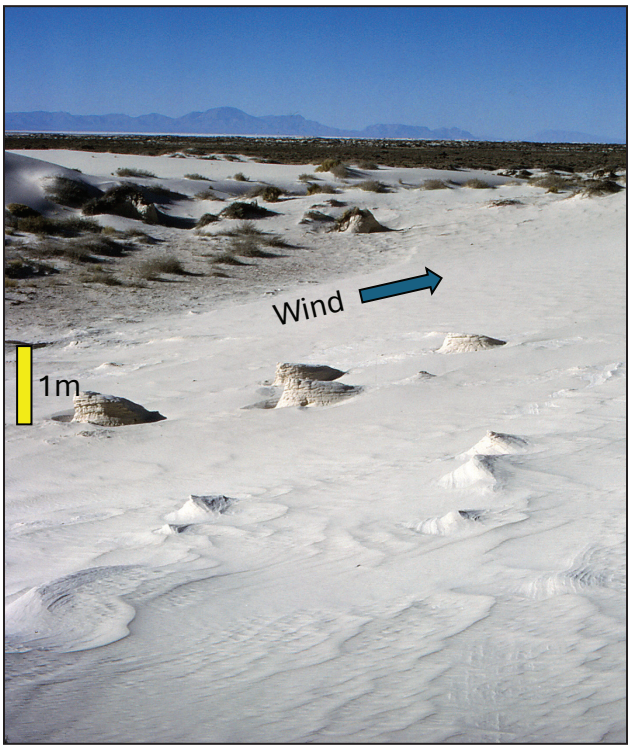

Figure 25. Small bedform (dune) micro-yardangs with typical rounded upwind prows tapering downwind to the right. Primary eolian strata, probably from the parabolic dune on which the photographer is standing, are etched on the surfaces of the yardangs. Moats have developed in front of the prows of several of these yardangs due to acceleration of wind around base of the yardang. View is toward the northwest.

Bedform yardangs, although conspicuous along shoreline trends mapped by Langford (1983), can form anywhere that cementation occurs within the dune sands. This habit differs from that of scarp yardangs, which most commonly form at slope breaks created by eolian scouring upwind of shoreline trends. This may be because cementation is caused both by the remobilization of gypsum by meteoric water, as described by Schenk and Fryberger (1988), as well as by processes peculiar to the shorelines of Lakes Otero and Lucero.

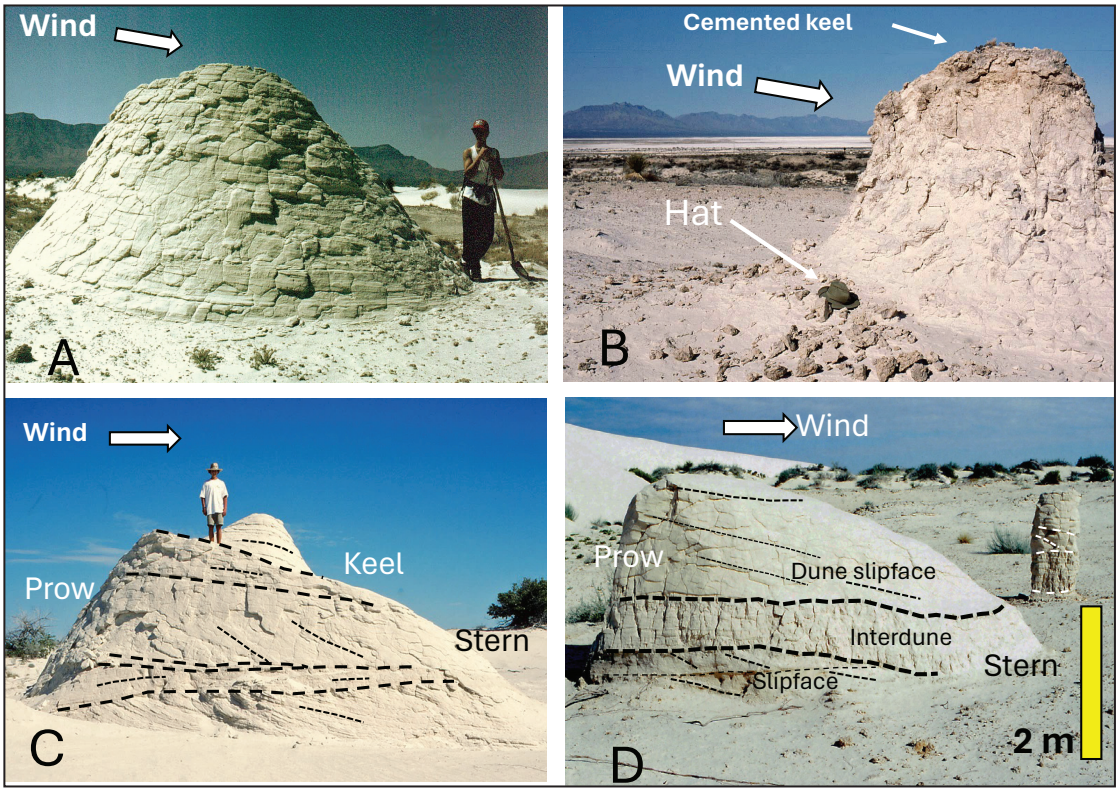

Figure 26. Bedform yardangs sculpted from early cemented portions of eolian dunes. (A) A yardang with low-angle eolian (ripple strata) cross-bedding, possibly formed from a parabolic dune that migrated downwind. The well-sculpted, "inverted boat hull" shape is typical of bedform yardangs at White Sands. Case hardening (cementation) of surface gypsum sand causes the slabby weathering aspect. (B) A bedform yardang near the NE 30 observation site (see Fig. 8 for the location of NE 30). This yardang has a brown, gypsum-cemented keel that has protected the underlying sediments, causing them to be streamlined by wind into a crude yardang. The yardang sediments themselves have been case hardened, falling off the sides as irregular plates. Pieces of the top protective layer are scattered around the base of this yardang. Hat for scale (marked by arrow). The Alkali Flat and San Andres Mountains are visible in the distance. (C) A large bedform yardang with a typical blunt prow that tapers downwind to a narrower stern. The steep cross-bedding within indicates that this yardang was largely sculpted from slipface deposits of the original dune. Some of the bounding surfaces and bedding are highlighted with dashed lines. Cross-bedding in the dune records the same southwest wind direction for the dune as that which formed the later yardang. View toward the north. (D) Peculiarities of yardang evolution. On the left is a perfectly streamlined yardang, composed of both dune slipface and interdune deposits. On the right is a columnar yardang with subdued streamlining in this view, although it is, in fact, slightly longer than wide.

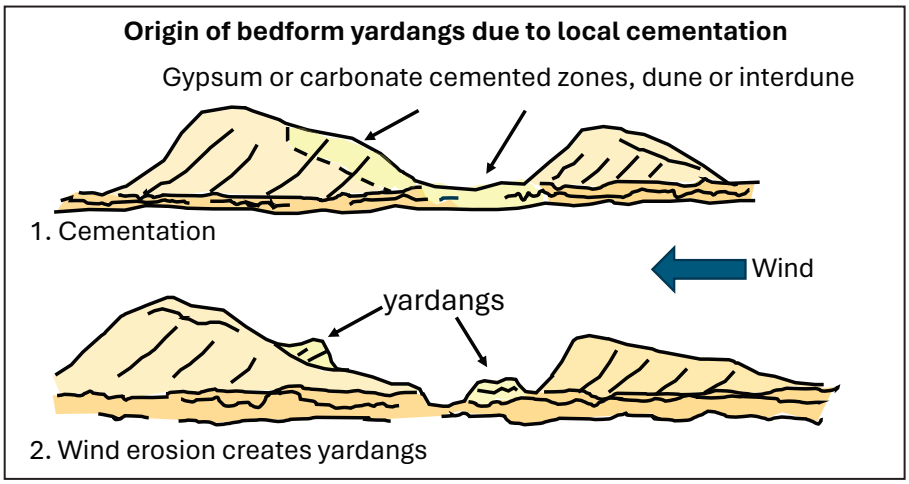

Figure 27. Bedform yardangs commonly form by wind streamlining of gypsum sand indurated by gypsum or carbonate cement within dunes and related sediments. Wavy flat lines and steeply dipping lines represent interdune bedding and dune cross-bedding, respectively.

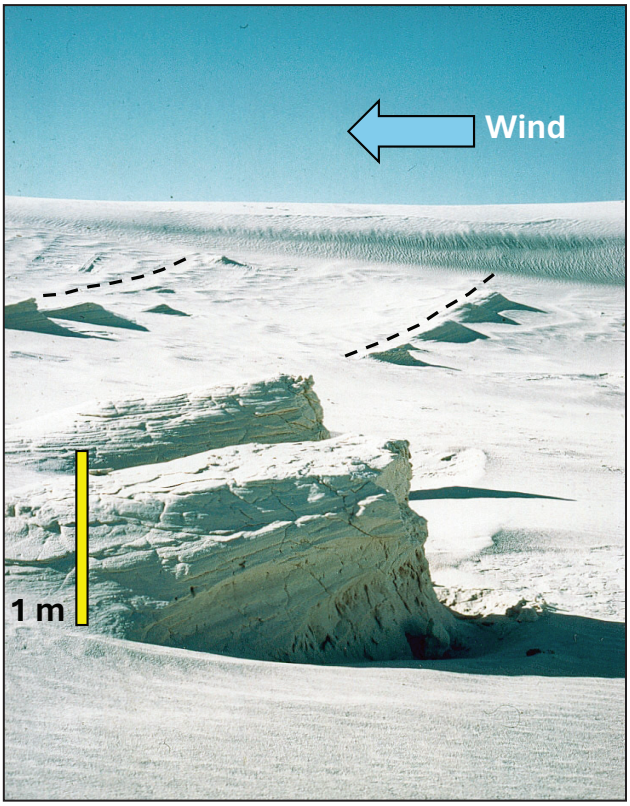

Figure 28. Small bedform yardangs on the windward slope of a barchanoid dune at White Sands National Park. They follow trends in cemented cross-bedding (the strike of cross-bedding is indicated by the dashed lines). Differential weathering (erosion) of cemented primary eolian strata is well exposed on the yardang in the foreground.

As mentioned above, bedform yardangs are also formed from wind scour and streamlining of interdune, sand sheet, and sabkha sediments (Fig. 29). This is because a rise in the water table may cause groundwater-based cementation of stratigraphically low facies such as interdunes and sand sheets. Subsequent lowering of the water table would expose the sediments to wind deflation and possibly lead to the carving of yardangs from the sediment. Interdune sediments at White Sands may also be cohesive due to early gypsum (or less commonly carbonate) cementation or due to dissolution and reprecipitation of gypsum by meteoric waters. The cementation is usually caused by the evaporation of saline waters of the capillary fringe and phreatic zones (Schenk and Fryberger, 1988). Interdune bedding is commonly flat or wavy, the latter aspect being the result of salt ridge growth during halite or perhaps gypsum crystal precipitation, primarily during the summer "evaporation season" (Fryberger et al., 1988).

Yardangs formed from interdune sediments tend to be small and irregular in profile, roughly streamlined and well-aligned with the southwest wind. Differential (fabric-selective) cementation of coarse- and fine-grained flat strata within the yardangs often results in the formation of wind-resistant ledges, sometimes with an undercut prow or a scour pit around the base of the yardang (Figs. 29 and 30).

Bedform yardangs formed from interdune sediments are often found in association with shrub yardangs created by saltcedar or plants that survive on meteoric or fresh groundwater stored in the sands of nearby dunes.

GEOMORPHOLOGY OF SHRUB YARDANGS

Shrub yardangs at White Sands evolve by wind scour of sediments cemented near the roots, rhizomes, or stems of shrubs, mostly of saltcedar, yucca, or other plants (Figs. 31 and 32). The process of cementation may be as simple as the removal of water by the roots, which concentrates solutes and causes deposition of gypsum cements (Owen et al., 2009). Gypsum is much less soluble in water than halite, and thus even partial evaporation of vadose pore water may precipitate dissolved gypsum. These cements, in turn, will be slow to dissolve when fresh rainwater again infiltrates the dune. Shrub yardangs are formed from previously deposited eolian dune or interdune sands above the groundwater table because these facies retain meteoric water. Thus, the colonizing plants have access to fresher water than on the Alkali Flat or other highly evaporitic terrains, such as evaporitic interdunes near the saline groundwater table in the dune field.

This process of formation of a shrub yardang differs from the formation of nebkhas, or coppice dunes. Nebkhas are created when drifting sand is trapped where vegetation slows the wind (Fig. 33). However, these forms can be transitional with each other.

Later stages of evolution of a nebkha can include partial erosion (Hesp and Smyth, 2019) that can thus cause them to evolve into very streamlined landforms. The key distinction is that, in most cases, the shrub yardangs we observed at White Sands were formed

from strata that were originally part of a freestanding dune rather than strata deposited around the plant as it grew (Fig. 34). We know this because we have trenched these features, as well as observed the original cross-bedding exposed on the surfaces of the shrub yardangs. Undoubtedly, however, there are overlapping processes of formation of pedestal dunes, shrub yardangs, and nebkhas. For more information on the evolution of nebkhas, see the discussion of Hesp and Smyth (2019) and their figure 7-3.

The term "shrub yardang" is a more accurate and useful term than "pedestal dune" at many localities in White Sands. This is because in many places the "pedestal dune" is not so much a kind of dune; rather, it is a yardang sculpted from a dune that moved onward due to biologically caused cementation. Moreover, the yardang, unlike a dune, is a geomorphic feature created by erosion, not deposition.

Shrub yardangs, as with other yardang types, evolve into streamlined forms that may persist long after the original plant has died and mostly decomposed. They can evolve into a yardang that shows little trace of the presence of a saltcedar or yucca. Careful study, however, should reveal bioturbation by roots and rhizomes, and thus the true origin of the yardang.

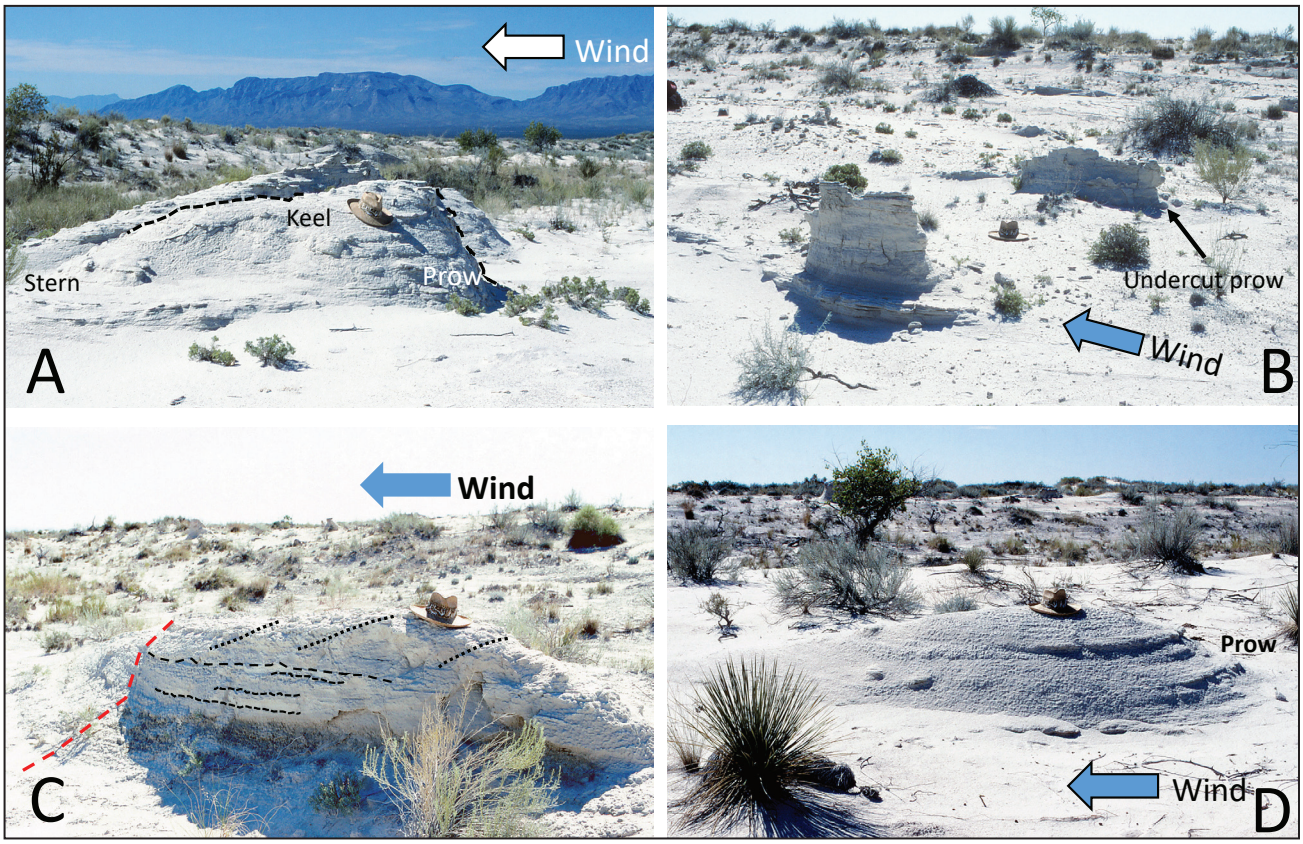

Figure 29. Small bedform yardangs in the interdune areas of parabolic dunes. (A) A small, well-streamlined "bedform" yardang. The flat bedding within indicates that dry, or perhaps originally damp, interdune sediments make up the yardang. The keel and prow of the foreground yardang are marked by a black dashed line. The prow is well rounded and tapers downwind along the keel to the stern. (B) Thin yardangs. The roughness of streamlining is the result of wind scour of horizontal strata that have different textures, and thus are unevenly cemented. The black arrow shows a yardang with an undercut prow, perhaps caused by saltating gypsum grains or differential weathering, followed by removal of fines by wind. The hat on the ground between the yardangs provides scale. (C) A yardang carved from slipface (avalanche) strata deposited over irregular interdune strata. The irregular beds below the topmost flat dashed line indicate a damp interdune, perhaps characterized by the presence of salt ridges. The cross-bedding above is also marked. As with many yardangs at White Sands, this one has an upper part with a steep side and a lower part with a more gently dipping side, as shown by the dashed red line. (D) A smooth, well-streamlined yardang eroded from flat-bedded eolian interdune sediments, mostly ripple strata. The ledges in the prow profile are due to differential cementation of layers within the yardang. View toward the southeast.

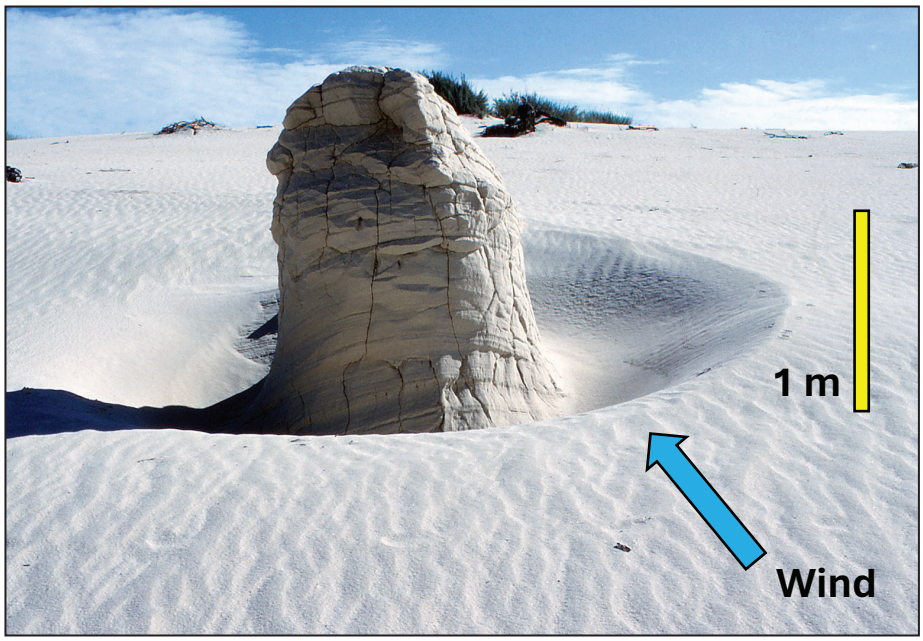

Figure 30. Scour pit around a bedform yardang. Scour moats are common where cemented sand is isolated within less-cemented or loose sand. Such moats may encircle the entire yardang, as shown here. Our field observations during sandstorms indicate that these scour pits are the result of vorticity around the base of the yardang. This vorticity increases wind speed near the ground on either side and in front of the yardang. Thus, sand that is less cemented is removed downwind, sculpting the yardang as it passes by.

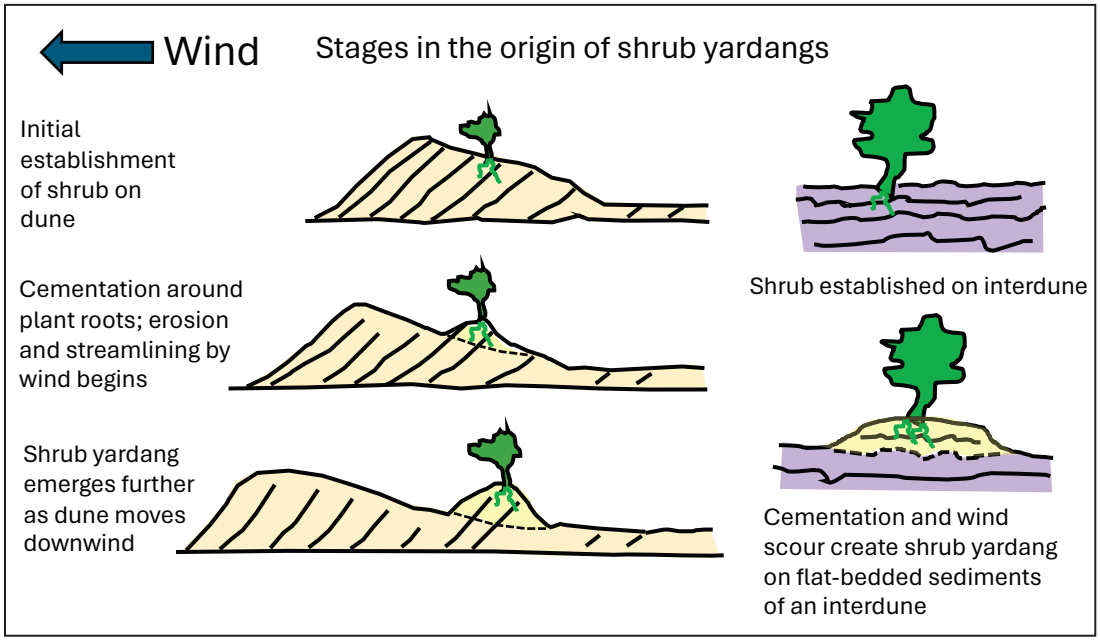

Figure 31. Stages in the origin of shrub yardangs. Although we show here a dune on which a woody plant has become established on the dune's windward slope, it is also possible that a plant can survive dune encroachment from upwind (for example, if dunes are small relative to the height of the plant). The result is similar, however, with cementation around the plant roots and rhizomes, and later formation of the shrub yardang.

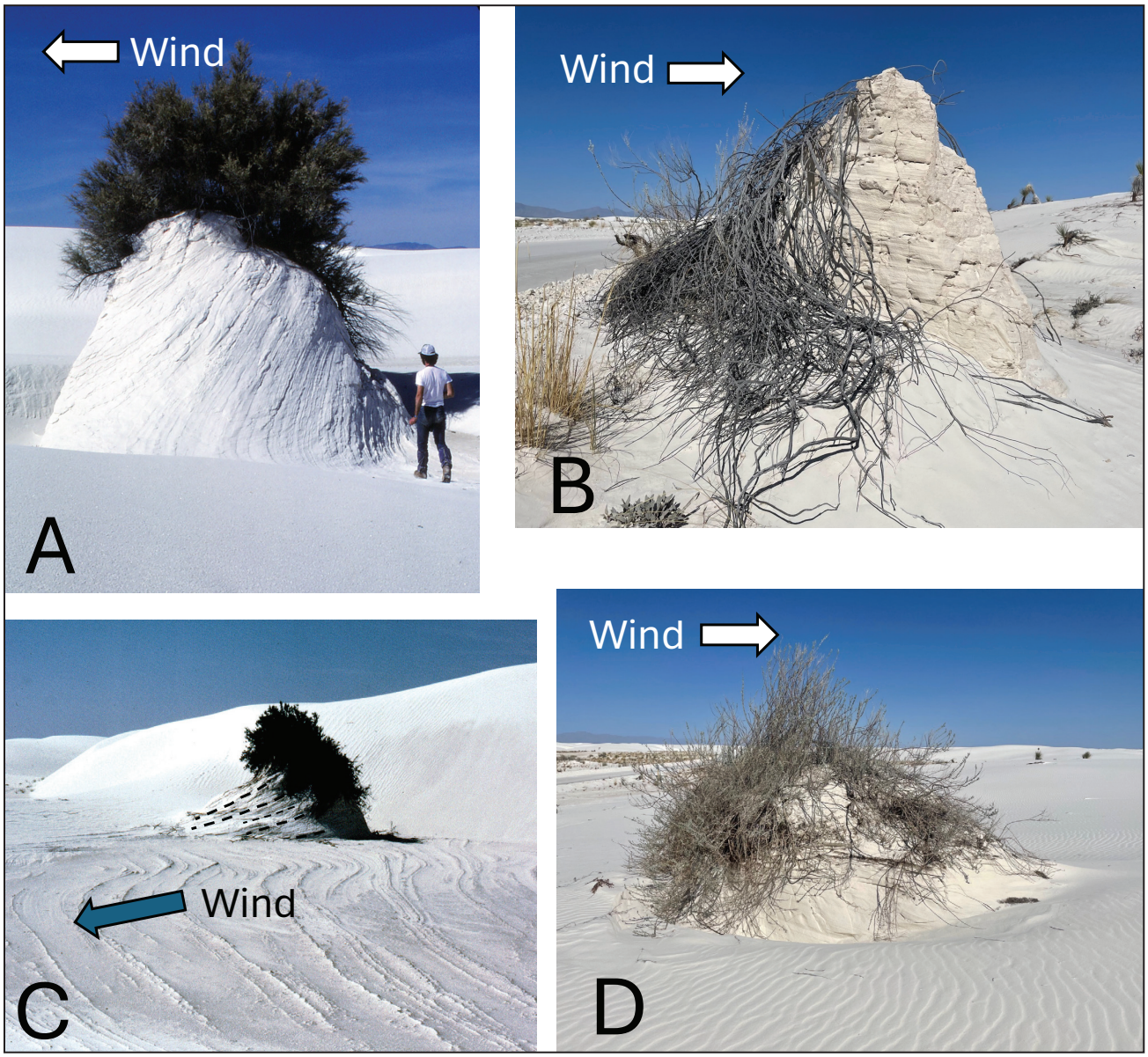

Figure 32. Examples of shrub yardangs at White Sands. (A) A well-streamlined shrub yardang in the interdune of a barchan dune. The dune on which this saltcedar originally grew has migrated on, leaving the shrub yardang, or "pedestal dune," as a freestanding form. (B) A shrub yardang built from sands cemented near saltcedar roots. The wind was obliquely from the left, as shown by the cross-bedding in the yardang. (C) A shrub yardang about 2 m high in an interdune. Dune cross-bedding in the yardang is highlighted by dashed lines. (D) A small shrub yardang in an open area of the barchanoid dune field.

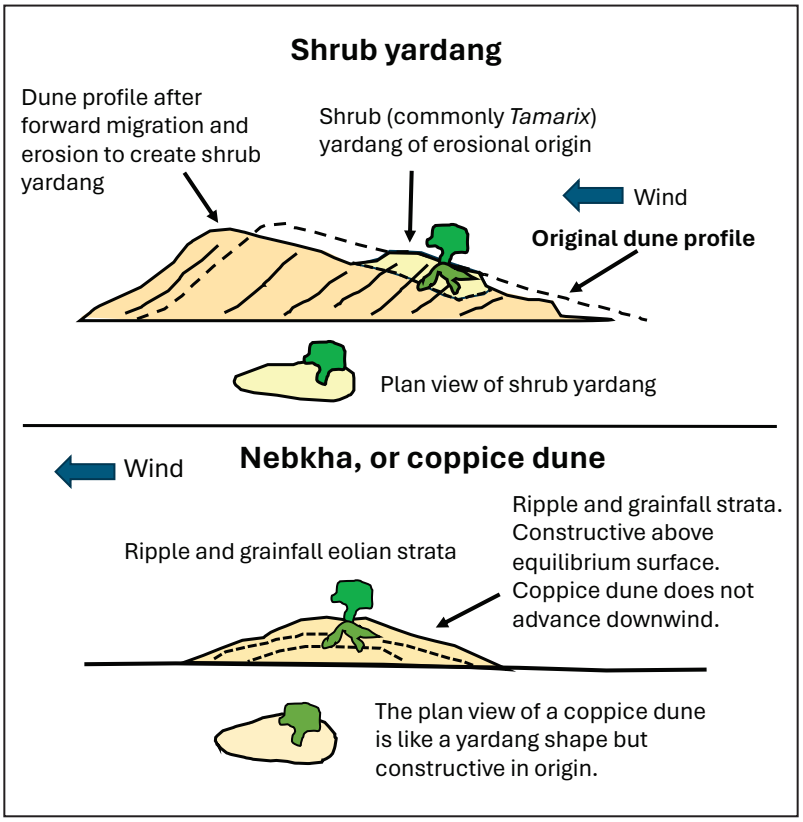

Figure 33. Distinguishing shrub yardangs (mostly erosional forms) from nebkha (coppice) dunes (mostly depositional forms).

Figure 34. A small nebkha (coppice dune; shown by black arrow) formed by the downwind settling of drifting sand in a sheltered zone caused by vegetation, Jafurah Sand Sea, Saudi Arabia. Shrub yardangs, on the other hand, are created when a saltcedar or other plant grows on a previously formed dune, preserving, rather than causing, sedimentation.

ANALYSIS OF YARDANG DIMENSIONS

Comparison of the White Sands Yardangs with Ideal Aerodynamic Form

It is of interest to compare our measurements of width-to-length ratio of the yardangs at White Sands with the ideal aerodynamic shape. An equilibrium form for a body immersed in a moving fluid has a width-to-length ratio of 1:4 (0.25), with a rounded upstream end and a tapered downstream end (Hughes and Brighton, 1967; Fox and McDonald, 1973).

There are two basic ways that yardang shapes diverge from the ideal: they are either too long or too short in length for a given width. If a yardang is too short, that is, unable to extend downwind, a lack of sufficient induration and thus rapid erosion may be the cause. On the other hand, in well-indurated sediments, such as bedrock or sandstone, yardangs that are aerodynamically mature (yet not perfectly streamlined) sometimes extend for many kilometers downwind. In any event, departure from the ideal shape is to be expected given the geological factors such as wind regime complexity, fluvial drainage patterns, and textural and sediment cementation processes, all of which play major roles in the formation of yardangs.

At White Sands, weak induration keeps the yardangs relatively short in length for a given width due to relatively rapid prow erosion. However, given this limitation, scarp yardangs in the northern study area 2 have width-to-length ratios rather close to the ideal of 0.25 for aerodynamic forms (Fig. 35A). This

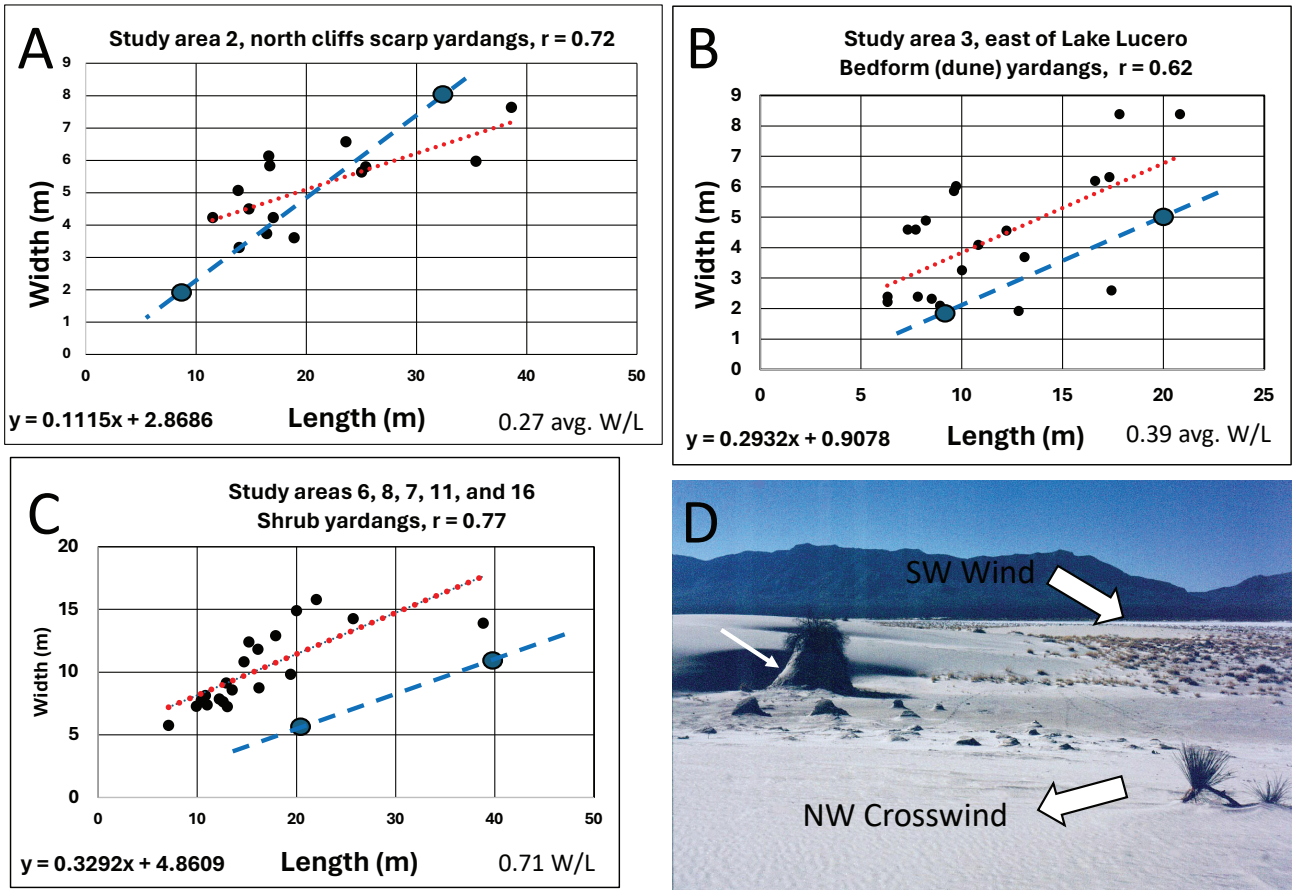

Figure 35. A comparison of width versus length values measured during this study, with an ideal streamlined object (0.25 width-to-length ratio). Dashed blue lines follow ideal shape, red dashed lines are the regression for the data. (A) Study area 2 scarp yardangs. (B) Study area 3 dune yardangs. (C) Study areas 6, 8, 7, 11, and 16 shrub yardangs. (D) This shrub yardang (white arrow on left), like most of those measured in Figure 35C, is too round to fit perfect aerodynamic streamlining. The small yardangs near the interdune appear to have formed in response to the northern component of the annual wind regime, perhaps due to sheltering from the southwest wind by the large dune on the left. The large shrub yardang may have formed from the dune on which the observer is standing. It is about to be overtaken by the succeeding dune. View toward the west. The fact that the height of this shrub yardang almost matches that of the nearby dune is further evidence that is not a nebkha, or coppice dune, most of which in this area are far smaller, like those in the background on the right.

may occur simply because they are eroded away on the upwind side about as fast as they form on the downwind side.

The dune yardangs in study area 3 (immediately east of Lake Lucero) fall somewhere between the scarp and shrub yardangs in terms of width-to-length ratio (Fig. 35B). Here the limiting factor would seem to be the size of the dune and its rate of downwind migration, as well as restricted areas of cemented zones in cross-bedded dunes and horizontally bedded facies such as interdunes and sand sheets. As noted above, extended forms are unlikely where induration is generally weak, as at White Sands.

On the other hand, shrub yardangs measured in several study areas have greater width with respect to length, possibly because they are dependent on plant growth processes that limit extension and thus diverge from the ideal substantially (Figs. 35C and 35D).

Comparison of the White Sands Yardangs with Each Other

There are distinctive groupings of yardang types at White Sands in terms of width-to-length ratio and other parameters (Fig. 36), simply in terms of physical size and shape and without respect to ideal forms. Shrub yardangs are the widest at White Sands, with width-to-length ratios from 0.5 to 8.5 (Fig. 36A). Bedform yardangs are thinner, with width-to-length ratios of 0.4 to 0.55. Scarp yardangs are the narrowest.

Exclusive of ratios, shrub yardangs at White Sands are the widest group, ranging from 8 to 16 m wide (Fig. 36B). Bedform yardangs are generally smaller in overall size than shrub yardangs and tend to have the narrowest measured widths recorded in this study at roughly 4 m. This occurs for the simple reason that bedform yardangs can be very

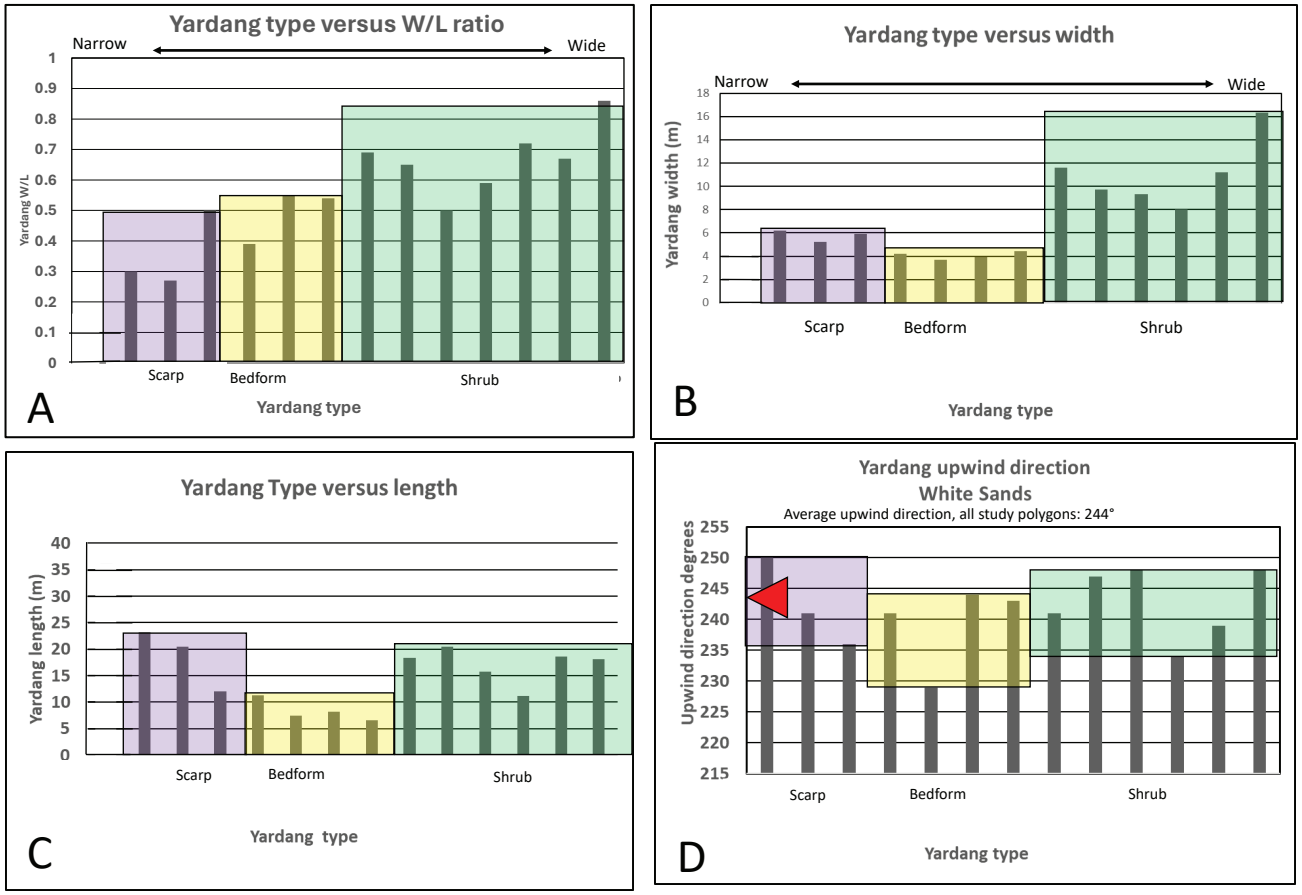

Figure 36. A summary of yardang measurements by type from all study areas and a summary of their orientation to the wind. (A) Yardang type versus width-to-length (W/L) ratio. (B) Yardang type versus width. (C) Yardang type versus length. (D) Indicated wind direction by yardang type. The red triangle indicates the average effective (upwind) direction.

small, down to the size of "micro" yardangs a few centimeters in width. Naturally, these small yardangs could not be measured from Google Earth imagery, which, although excellent, was accurate to roughly 0.5 m resolution. Scarp yardangs fall between shrub and bedform yardangs in width.

Scarp yardangs at White Sands average from 12 to 25 m in length among the three areas where they were measured (study areas 1, 2, and 15; Fig. 36C). Shrub yardangs can be surprisingly long, due mainly to their large size, although proportions are rounder than scarp yardangs. Dune yardangs at White Sands are generally the shortest, seldom having enough cementation, protection from erosion by hard layers in the sediment, or growing plants to resist wind erosion for long.

All yardang types at White Sands are aligned closely, but seldom exactly, to the resultant drift direction of the effective winds as computed from nearby Holloman AFB (Fig. 36D; see also Figs. 8 and 17). The red triangle in Figure 36D indicates the average upwind direction of all yardangs studied at White Sands for graphic comparison with the range of orientation to wind of the various yardang types. The weakest match to regional winds are the bedform yardangs, perhaps a result of deflection of wind direction by the dunes and sheltering effects.

DISCUSSION OF RESULTS

YARDANGS AND THE HISTORY OF LAKE OTERO

The yardangs at White Sands record an important and ongoing chapter in the story of the shallow, evaporitic basin formerly occupied by Lake Otero. After the lake dried, the surficial basin was deepened by wind scour. This scour was regulated by an episodically declining water table beginning in the Holocene, perhaps around 15.5 ka, and extending to the present day (see Allen et al. [2009], p. 18–19, for a comprehensive discussion). The sand-sized crystals released by wind erosion became the White Sands dune field. The boundary between the wind-formed basin carved into sediments of former Lake Otero and the marginally higher ground makes up portions of the various shorelines described and mapped by previous workers (Langford, 2003; Kocurek et al., 2007; Allen et al., 2009). This process is thought by most workers to be responsible, at least in part, for the creation of terraces at still-stands of the underlying shallow groundwater water table that, in turn, limited the depth of scour on the Alkali Flat (Fig. 37). Conventional lacustrine shorelines, represented by lake-margin dunes or lunettes from former Lake Otero highstands, are also present around White Sands (Allen et al., 2009). They are clearly visible in Google Earth imagery, particularly in the southern part of White Sands National Park.

FAMILIES OF YARDANGS AND THEIR MORPHOLOGICAL EVOLUTION

In this study, we have observed and informally named three yardang types at White Sands based on distinctive local processes of formation: *bedform*, *scarp*, and *shrub*. A more "global" terminology for yardangs has been used by other authors, grouping them into the families of *stationary*, *translational*, and *extensional* types. Our terms fit into the *stationary* (*bedform* and *shrub*) and *translational* (*scarp*) types, while *extensional* yardangs are not present at White Sands.

The extensional yardang family, as illustrated in Figure 4, includes yardangs with far greater length than the scarp yardangs that, certainly at White Sands, tend to merge into higher terrain downwind within tens of meters. Extensional yardangs such as those in Iran and Egypt may indeed have upwind scarps, but in many places these yardangs commonly extend many kilometers downwind (Goudie, 2007). We do not know if the elongate aspect (extension) of any yardang field must originate from propagation downwind from a scarp, for instance, or as part of some continuous process of wind erosion along the entire length—controlled in part by vorticity, for example. Perhaps these features form by a combination of both processes. Certainly, the various families of yardangs can evolve from one family into another over time, or through a change in process framework; for example, changes in precipitation or wind regime. In any event, it is not clear to us whether the shape of extensional yardangs represents an outcome of self-organizing behavior independent of scarps that may lie upwind, or a dynamic evolution downwind that alters the spacing or shape of the scarp yardangs that presumably formed first.

OTHER DESCRIPTIVE TERMS FOR YARDANG FAMILIES

The classification of yardangs has been addressed by previous workers using various approaches, which we summarize below. The terminology derives from various aspects of yardang evolution in settings around the world, including growth habit, size, shape, geomorphology, and age. Of course, many geological and environmental factors will influence the formation of yardangs in any region, including sedimentary geology, structure, wind regime, and precipitation, to name a few. We recognize that our suggestions for the assignment of White Sands yardangs to any classification beyond White Sands is necessarily imperfect; however, we do this to highlight the growth processes of the White Sands yardangs.

To illustrate the variety of available approaches to classifying yardangs, we list below a selection of ideas proposed by other workers.

Growth habit: (This report). Stationary, translational, and extensional (Fig. 4).

Size: Cooke et al. (1993) and Laity (2009). Micro-yardangs (less than 4 m long), meso-yardangs (4–10 m high, 100+ m long), and mega-yardangs (10–200+ m high, many km long).

Shape (width-to-length ratio): Hu et al. (2017). Short axis (1:2), whale-back (2:6), hogsback (6:10), and long-ridge (10:210). Context is important, including geological setting, bedding orientation, structural position, and lithologic heterogeneity.

Geomorphology: Li et al. (2016). These authors recognize and provide measurements of long-ridge yardangs (20–1,702 m length), mesa and small-ridge yardangs (11–409 m length), and whaleback and saw-tooth crested yardangs (39–575 m length), along with statistical summaries of shape.

Age: Ding et al. (2020) recognize embryonic, juvenile, mature, and demise stages of growth and removal by wind erosion, with classification based on stage of evolution, independent of time considerations.

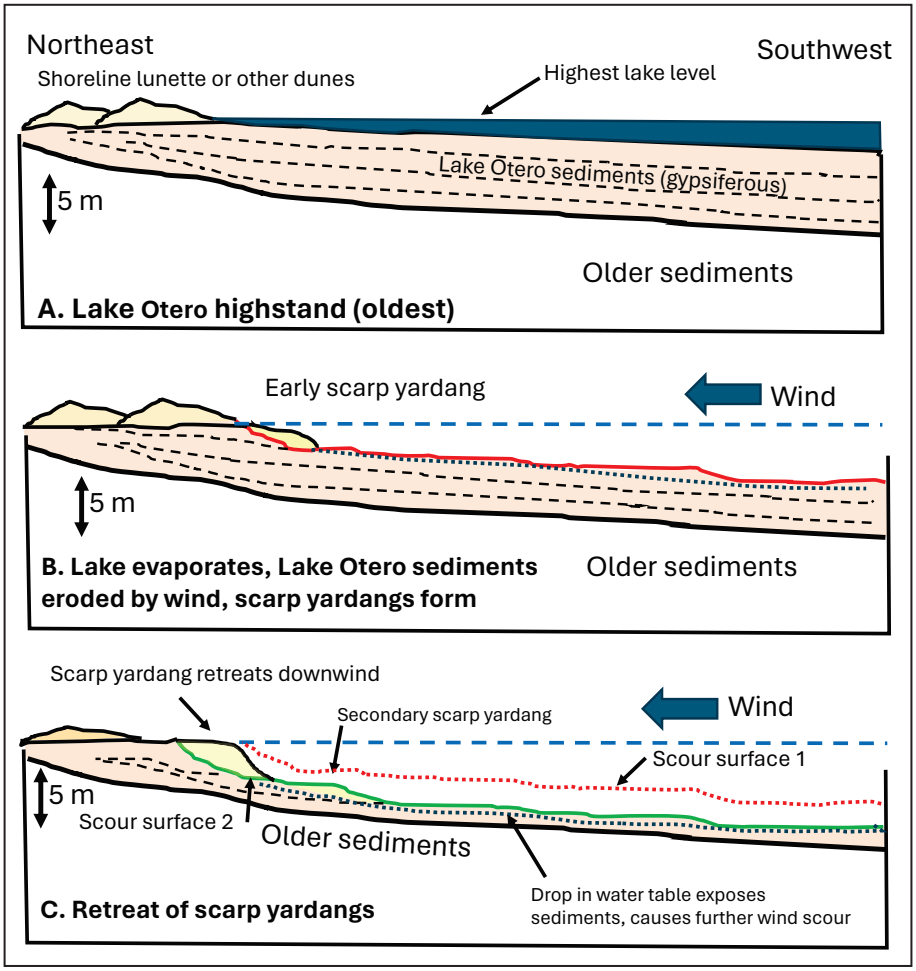

Figure 37. Schematic geological cross sections showing the origin of scarp yardangs at White Sands. (A) The climate became increasingly hot and evaporitic in the early Holocene after the ultimate highstand at 1,204 m (Allen et al., 2009). Gypsiferous sediments were deposited, with lake margin lunettes or other dunes building up along the shoreline as the lake dried (episodically). (B) Scarp yardangs formed following fluvial gullying of a gently rising slope formed by wind scour of the Alkali Flat. A cliff emerged, held up by case hardening of surficial sediments, coarse sediments that resisted wind erosion, or both. The relief of the cliff increased as wind erosion of the Alkali Flat continued down to the level of a falling near-surface water table (shown by dotted blue line). (C) The scarp yardangs retreated downwind as scour of the Alkali Flat continued.

CONCLUSIONS

White Sands hosts a wide range of sizes and shapes for erosional features that we recognize as yardangs. The shape of a yardang at White Sands is dependent on the interaction of wind erosion with complex geological settings and processes (including both eolian and fluvial processes).

Three types of yardangs are recognized at White Sands, informally referred to here as *scarp, bedform*, and *shrub* yardangs. *Scarp* yardangs are mostly distributed along paleoshorelines or scarps on the downwind margin of the Alkali Flat. These yardangs are commonly shaped from interfluves cut into the moderately indurated and commonly gypsiferous sediments of ancient Lake Otero or modern Lake Lucero. They tend to translate downwind as the shorelines erode. *Bedform* yardangs are formed from early cemented sediments of eolian dune bedforms and associated facies such as interdunes, sand sheets, and eolian sabkhas. *Shrub* yardangs at White Sands are formed from erosion and streamlining of sediments cemented around the roots and rhizomes of saltcedar shrubs and yuccas.

Our measurements using satellite imagery and ground photographs document a wide range of sizes and shapes for yardangs at White Sands, few of which fit the ideal 1:4 ratio of width to length expected with perfect aerodynamic streamlining. Nevertheless, correlation coefficients of width to length are impressively high, suggesting a common control of yardang shape by the action of wind, as modified by geology.

In general, the yardangs at White Sands are aligned parallel to the resultant drift direction of the wind regime at Holloman AFB (064°, roughly toward the northeast, meaning wind from the southwest from 244°). The sand roses also show subsidiary sand drift from the northwest (winter) and southeast (summer) that may explain some smaller yardangs that deviate from the regional southwest wind, where the dominant southwest wind is blocked by dunes.

The yardangs at White Sands have formed in a low- to moderate-energy wind regime. This may have been possible due to the generally weak induration of sediments making up the yardangs, thus creating a greater susceptibility to wind streamlining than sediments elsewhere that are more indurated.

Finally, most yardangs at White Sands are carved from dominantly gypsiferous sediments of fluvial, lacustrine, or eolian origin. The cohesion required to form these yardangs commonly exists where sediments have been cemented by the following processes: (a) precipitation of evaporite cements in proximity to a saline groundwater table, (b) dissolution and reprecipitation of gypsum by meteoric waters, or (c) precipitation of evaporite cements (mainly gypsum) around plant roots or rhizomes.

REFERENCES CITED

Allen, B.D., 1994, Ancient lakes—A tool for understanding climatic change: Lite Geology, v. 8, summer 1994, p. 8–10.

Allen, B.D., 2005, Ice age lakes in New Mexico, *in* Lucas, S.G., Morgan, G.S., and Zeigler, K.E., eds., New Mexico's Ice Ages: New Mexico Museum of Natural History and Science Bulletin 28, p. 107–114.

Allen, B.D., and Anderson, R.Y., 2000, A continuous, high-resolution record of late Pleistocene climate variability from the Estancia Basin, New Mexico: Geological Society of America Bulletin, v. 112, no. 9, p. 1444–1458. https://doi.org/10.1130/0016-7606(2000)112%3C1444:ACHRRO%3E2.0.CO;2

Allen, B.D., Love, D.W., and Myers, R.G., 2006, Preliminary age of mammal footprints in Pleistocene lake-margin sediments of the Tularosa Basin, south-central New Mexico [abstract]: New Mexico Geological Society Annual Spring Meeting, April 21, 2006, Macy Center, New Mexico Institute of Mining and Technology, Socorro, NM. https://doi.org/10.56577/SM-2006.970

Allen, B.D., Love, D.W., and Myers, R.G., 2009, Evidence for late Pleistocene hydrologic and climatic change from Lake Otero, Tularosa Basin, south-central New Mexico: New Mexico Geology, v. 31, no. 1, p. 9–25. https://doi.org/10.58799/NMG-v31n1.9

Allmendinger, R.J., 1971, Preliminary evaluation of the role of the hydrologic cycle in the development of the white sands, White Sands National Monument, New Mexico: Geological Society of America, Abstracts with Programs, v. 3, p. 231–232.

Allmendinger, R.J., 1972, Hydrologic control over the origin of gypsum at Lake Lucero, White Sands National Monument, New Mexico [MS thesis]: Socorro, New Mexico Institute of Mining and Technology, 182 p.

Allmendinger, R.J., and Titus, F.B., 1973, Regional hydrology and evaporative discharge as present-day source of gypsum at White Sands National Monument, New Mexico: New Mexico Bureau of Mines and Mineral Resources Open-File Report 55, 26 p. https://doi.org/10.58799/OFR-55

Baitis, E., Kocurek, G., Smith, V., Mohrig, D., Ewing, R.C., and Peyret, A.-P.B., 2014, Definition and origin of the dune-field pattern at White Sands, New Mexico: Aeolian Research, v. 15, p. 269–287. https://doi.org/10.1016/j.aeolia.2014.06.004

Basabilvazo, G.T., and Myers, R.G., 1994, Geohydrology of the High Energy Laser System Test Facility site, White Sands Missile Range, Tularosa Basin, south-central New Mexico: U.S. Geological Survey Water Resources Investigations Report 93-4192, 59 p. https://doi.org/10.3133/wri934192

Bennett, M.R., Bustos, D., Belvedere, M., Martinez, P., Reynolds, S.C., and Urban, T., 2019, Soft-sediment deformation below mammoth tracks at White Sands National Monument (New Mexico) with implications for biomechanical inferences from tracks: Palaeogeography, Palaeoclimatology, Palaeoecology, v. 527, p. 25–38. https://doi.org/10.1016/j.palaeo.2019.04.023

Bennett, M.R., Bustos, D., Odess, D., Urban, T.M., Lallensack, J.N., Budka, M., Santucci, V.L., Martinez, P., Wiseman, A.L.A., and Reynolds, S.C., 2020, Walking in mud—Remarkable Pleistocene human trackways from White Sands National Park (New Mexico): Quaternary Science Reviews, v. 249, 106610. https://doi.org/10.1016/j.quascirev.2020.106610

Bennett, M.R., et al., 2021, Evidence of humans in North America during the last glacial maximum: Science, v. 373, no. 6562, p. 1528–1531. https://doi.org/10.1126/science.abg7586

Blackwelder, E., 1934, Yardangs: Geological Society of America Bulletin, v. 45, no. 1, p. 159–166. https://doi.org/10.1130/GSAB-45-159

Bosworth, T.O., 1922, Work of wind in the desert (part 4, chapter 4), *in* Geology of the Tertiary and Quaternary Periods in the North-West Part of Peru: London, Macmillan and Co. Ltd., p. 293–311.

Breed, C.S., Fryberger, S.G., Andrews, S., McCauley, C., Lennartz, F., Gebel, D., and Horstman, K., 1979, Chapter K—Regional studies of sand seas using Landsat (ERTS) imagery, *in* McKee, E.D., ed., A study of global sand seas: U.S. Geological Survey Professional Paper 1052, p. 305–399. https://doi.org/10.3133/pp1052

Breed, C.S., Embabi, N.S., El-Etr, H.A., and Grolier, M.J., 1980, Wind deposits in the western desert: The Geographical Journal, v. 146, no. 1, p. 88–90. https://doi.org/10.2307/634078

Breed, C.S., McCauley, J.F., and Grolier, M.J., 1982, Relict drainages, conical hills, and the eolian veneer in southwest Egypt—Applications to Mars: Journal of Geophysical Research, v. 87, no. B12, p. 9929–9950. https://doi.org/10.1029/JB087iB12p09929

Breed, C.S., McCauley, J.F., and Whitney, M.I., 1989, Wind erosion forms, *in* Thomas, D.S.G., ed., Arid Zone Geomorphology, p. 284–307.

Brook, G.A., 2002, Yardangs in ancient, reddened eolian sands south of Mogadishu, Somalia: The Arab World Geographer, v. 5, no. 3, p. 141–155.

Buck, B., 1996, Late Quaternary landscape evolution, paleoclimate, and geoarchaeology, southern New Mexico and West Texas [PhD thesis]: Las Cruces, New Mexico State University, 382 p.

Bustos, D., et al., 2018, Footprints preserve terminal Pleistocene hunt?—Human-sloth interactions in North America: Science Advances, v. 4, no. 4, eaar7621. https://doi.org/10.1126/sciadv.aar7621

Connell, S.D., Hawley, J.W., and Love, D.W., 2005, Late Cenozoic drainage development in the southeastern Basin and Range of New Mexico, southeasternmost Arizona, and western Texas, *in* Lucas, S.G., Morgan, G.S., and Ziegler, K.E., eds., New Mexico's Ice Ages: New Mexico Museum of Natural History and Science Bulletin 28, p. 125–150.

Cooke, R., Warren, A., and Goudie, A.S., 1993, Desert Geomorphology (revised edition): London, UCL Press, 526 p.

de Silva, S.L., Bailey, J.E., Mandt, K.E., and Viramonte, J.M., 2010, Yardangs in terrestrial ignimbrites—Synergistic remote and field observations on Earth with applications to Mars: Planetary and Space Science, v. 58, no. 4, p. 459–471. https://doi.org/10.1016/j.pss.2009.10.002

Ding, Z., Zhao, J., Wang, J., and Lai, Z., 2020, Yardangs on Earth and implications to Mars—A review: Geomorphology, v. 364, 107230. https://doi.org/10.1016/j.geomorph.2020.107230

El-Baz, F., 2001, Gifts of the desert: Archaeology, v. 54, no. 2, p. 42–45. https://www.jstor.org/stable/41779395

El-Baz, F., Breed, C.S., Grolier, M.J., and McCauley, J.F., 1979, Eolian features in the Western Desert of Egypt and some applications to Mars: Journal of Geophysical Research, v. 84, no. B14, p. 8205–8221. https://doi.org/10.1029/JB084iB14p08205

Ewing, R.C., 2020, White Sands, *in* Lancaster, N., and Hesp, P., eds., Inland Dunes of North America: Cham, Switzerland, Springer Nature, p. 207–237.

Ewing, R.C., and Kocurek, G.A., 2010, Aeolian dune interactions and dune-field pattern formation—White Sands Dune Field, New Mexico: Sedimentology, v. 57, no. 5, p. 1199–1219. https://doi.org/10.1111/j.1365-3091.2009.01143.x

Favaro, E.A., Hugenholtz, C.H., and Barchyn, T.E., 2021, Antecedent controls on the spatial organization of yardangs on the Puna Plateau, north-western Argentina: Earth Surface Processes and Landforms, v. 46, no. 15, p. 3063–3077. https://doi.org/10.1002/esp.5212

Fox, R.W., and McDonald, A.T., 1973, Introduction to Fluid Mechanics: New York, John Wiley & Sons, 630 p.

Fryberger, S.G., 2001a, Geological overview of White Sands National Monument: National Park Service (legacy web document).

Fryberger, S.G., 2001b, Reconnaissance geomorphic map of the White Sands Dune Field, New Mexico, *in* KellerLynn, K., 2012, White Sands National Monument, Geologic Resources Inventory Report: National Park Service NPS/NRSS/GRD/NRR—2012/585.

Fryberger, S.G., and Dean, G., 1979, Dune forms and wind regime, *in* McKee, E.D., ed., A study of global sand seas: U.S. Geological Survey Professional Paper 1052, p. 137–169. https://doi.org/10.3133/pp1052

Fryberger, S.G., and Ormerod, S.F., 2023, A geological overview of White Sands National Park, New Mexico, USA (second edition): Researchgate.net, 139 p. http://dx.doi.org/10.13140/RG.2.2.34758.45127

Fryberger, S.G., Al-Sari, A.M., and Clisham, T.J., 1983, Eolian dune, interdune, sand sheet, and siliciclastic sabkha sediments of an offshore prograding sand sea, Dhahran Area, Saudi Arabia: American Association of Petroleum Geologists Bulletin, v. 67, no. 2, p. 280–312. https://doi.org/10.1306/03B5ACFF-16D1-11D7-8645000102C1865D

Fryberger, S.G., Al-Sari, A.M., Clisham, T.J., Rizvi, S.A.R., and Al-Hinai, K.G., 1984, Wind sedimentation in the Jafurah sand sea, Saudi Arabia: Sedimentology, v. 31, no. 3, p. 413–431. https://doi.org/10.1111/j.1365-3091.1984.tb00869.x

Fryberger, S.G., Schenk, C.J., and Krystinik, L.F., 1988, Stokes surfaces and the effects of near-surface groundwater-table on eolian deposition: Sedimentology, v. 35, no. 1, p. 21–41. https://doi.org/10.1111/j.1365-3091.1988.tb00903.x

Ghodsi, M., 2017, Morphometric characteristics of yardangs in the Lut Desert, Iran: Desert, v. 22, no. 1, p. 21–29. https://doi.org/10.22059/jdesert.2017.62251

Goudie, A.S., 2007, Mega-yardangs—A global analysis: Geography Compass, v. 1, no. 1, p. 65–81. https://doi.org/10.1111/j.1749-8198.2006.00003.x

Goudie, A.S., 2008, The history and nature of wind erosion in deserts: Annual Review of Earth and Planetary Sciences, v. 36, p. 97–119. https://doi.org/10.1146/annurev.earth.36.031207.124353

Grolier, M.J., McCauley, J.F., Breed C.S., and Embabi, N.S., 1980, Yardangs of the Western Desert: The Geographical Journal, v. 146, no. 1, p. 86–87. https://doi.org/10.2307/634077

Gutiérrez-Elorza, M., Desir, G., and Gutiérrez-Santolalla, F., 2002, Yardangs in the semiarid central sector of the Ebro Depression (NE Spain): Geomorphology, v. 44, no. 1–2, p. 155–170. https://doi.org/10.1016/S0169-555X(01)00151-9

Hedin, S., 1905, Scientific Results of a Journey in Central Asia 1899–1902, Vol. II—Lop-Nor: Stockholm, Lithographic Institute of the General Staff of the Swedish Army, 717 p.

Herrick, C.L., 1904, Lake Otero, an ancient salt lake in southeastern New Mexico: The American Geologist, v. 34, p. 174–189.

Hesp, P.A., and Smyth, T.A.G., 2019, Anchored dunes, *in* Livingstone, I., and Warren, A., eds., Aeolian Geomorphology—A New Introduction (first edition): Hoboken, New Jersey, Wiley–Blackwell, 336 p.

Holliday, V.T., Cuba, M., Lee, W., Windingstad, J., Fenerty, B., and Bustos, D., 2023, Onset of dune construction based on archaeological evidence, White Sands, New Mexico: Quaternary Research, v. 115, p. 1–9. https://doi.org/10.1017/qua.2023.22

Hu, C., Chen, N., Kapp, P., Chen, J., Xiao, A., and Zhao, Y., 2017, Yardang geometries in the Qaidam Basin and their controlling factors: Geomorphology, v. 299, p. 142–151. https://doi.org/10.1016/j.geomorph.2017.09.029

Hughes, W.F., and Brighton, J.A., 1967, Fluid Dynamics: New York, Schaum, 265 p.

Iowa State University Environmental Mesonet, 2024, Wind roses: https://mesonet.agron.iastate.edu/sites/windrose.phtml?station=4MY&network=NM_ASOS

Jones, L.S., and Blakey, R.C., 1993, Erosional remnants and adjacent unconformities along an eolian-marine boundary of the Page Sandstone and Carmel Formation, Middle Jurassic, south-central Utah: Journal of Sedimentary Petrology, v. 63, p. 852–859. https://doi.org/10.1306/D4267C26-2B26-11D7-8648000102C1865D

KellerLynn, K., 2012, White Sands National Monument—Geologic Resources Inventory Report: National Park Service Natural Resource Report NPS/NRSS/GRD/NRR–2012/585, 100 p.

Kerber, L., and Head, J.W., 2010, The age of the Medusae Fossae Formation—Evidence of Hesperian emplacement from crater morphology, stratigraphy, and ancient lava contacts: Icarus, v. 206, no. 2, p. 669–684. https://doi.org/10.1016/j.icarus.2009.10.001

Kocurek, G., Carr, M., Ewing, R., Havholm, K., Nagar, Y.C., and Singhvi, A.K., 2007, White Sands Dune Field, New Mexico—Age, dune dynamics and recent accumulations: Sedimentary Geology, v. 197, no. 3–4, p. 313–331. https://doi.org/10.1016/j.sedgeo.2006.10.006

Kottlowski, F.E., 1958, Lake Otero—Second phase in formation of New Mexico's gypsum dunes: Geological Society of America Bulletin, v. 69, p. 1733–1734.

Laity, J.E., 2009, Landforms, landscapes, and processes of eolian erosion, *in* Parsons, A.J., and Abrahams, A.D., eds., Geomorphology of Desert Environments (second edition): Dordrecht, Netherlands, Springer Science+Business Media B.V., p. 597–627.

Langford, R.P., 2003, The Holocene history of the White Sands dune field and influences on eolian deflation and playa lakes: Quaternary International, v. 104, p. 31–39. https://doi.org/10.1016/S1040-6182(02)00133-7

Langford, R.P., Rose, J.M., and White, D.E., 2009, Groundwater salinity as a control on development of eolian landscape—An example from the White Sands of New Mexico: Geomorphology, v. 105, no. 1–2, p. 39–49. https://doi.org/10.1016/j.geomorph.2008.01.020

Li, J., Dong, Z., Qian, G., Zhang, A., Luo, W., Lu, J., and Wang, M., 2016, Yardangs in the Qaidam Basin, northwestern China—Distribution and morphology: Aeolian Research, v. 20, p. 89–99. https://doi.org/10.1016/j.aeolia.2015.11.002

Mamer, E., and Newton, B.T., 2017, The relationship between the Cuatrociénegas gypsum dune field and the regional hydrogeology, Coahuila, Mexico: New Mexico Bureau of Geology and Mineral Resources Open-File Report 589, 35 p. https://doi.org/10.58799/OFR-589

McCauley, J.F., 1973, Mariner 9 evidence for wind erosion in the equatorial and mid-latitude regions of Mars: Journal of Geophysical Research, v. 78, no. 20, p. 4123–4137. https://doi.org/10.1029/JB078i020p04123

McCauley, J.F., Grolier, M.J., and Breed, C.S., 1977a, Yardangs of Peru and other desert regions: U.S. Geological Survey Interagency Report Astrogeology 81, 177 p.

McCauley, J.F., Breed, C.S., and Grolier, M.J., 1977b, Yardangs, *in* Doehring, D.O., ed. Geomorphology in Arid Regions: London, George Allen and Unwin Ltd., p. 233–269.

McCauley, J.F., Breed, C.S., El-Baz, F., Whitney, M.I., Grolier, M.J., and Ward, A.W., 1979, Pitted and fluted rocks in the Western Desert of Egypt—Viking Comparisons: Journal of Geophysical Research, v. 84, no. B14, p. 8222–8232. https://doi.org/10.1029/JB084iB14p08222

McKee, E.D., 1966, Structures of dunes at White Sands National Monument, New Mexico (and a comparison with structures of dunes from other selected areas): Sedimentology, v. 7, no. 1, p. 3–69. https://doi.org/10.1111/j.1365-3091.1966.tb01579.x

McKee, E.D., and Douglass, J.R., 1971, Growth and movement of dunes at White Sands National Monument, New Mexico: U.S. Geological Survey Professional Paper 0750-D, p. D108–D114. https://doi.org/10.3133/pp750D

McKee, E.D., and Moiola, R.J., 1975, Geometry and growth of the White Sands dune field, New Mexico: Journal of Research of the U.S. Geological Survey, v. 3, no. 1, p. 59–66. https://doi.org/10.3133/70007406

McLean, J.S., 1970, Saline ground-water resources of the Tularosa Basin, New Mexico: Open File Report prepared in cooperation with the New Mexico State Engineer and the Office of Saline Water, Department of the Interior, OSW Agreement No. 14-01-0001-2091, 139 p.

Newton, B.T., and Allen, B., 2014, Hydrologic investigation at White Sands National Monument: New Mexico Bureau of Geology and Mineral Resources Open-File Report 559, 51 p. https://doi.org/10.58799/OFR-559

Owen, R.B., Renaut, R.W., Scott, J.J., Potts, R., and Behrensmeyer, A.K., 2009, Wetland sedimentation and associated diatoms in the Pleistocene Olorgesailie Basin, southern Kenya Rift Valley: Sedimentary Geology, v. 222, no. 1–2, p. 124–137. https://doi.org/10.1016/j.sedgeo.2009.03.013

Pelletier, J.D., Kapp, P.A., Abell, J., Field, J.P., Williams, Z.C., and Dorsey, R.J., 2018, Controls on yardang development and morphology—1. Field observations and measurements at Ocotillo Wells, California: Journal of Geophysical Research–Earth Surface, v. 123, no. 4, p. 694–722. https://doi.org/10.1002/2017JF004461

Rachal, D.M., Zeigler, K., Dello-Russo, R., and Solfisburg, C., 2021, Lake levels and trackways—An alternative model to explain the timing of human-megafauna trackway intersections, Tularosa Basin, New Mexico: Quaternary Science Advances, v. 3, 100024. https://doi.org/10.1016/j.qsa.2021.100024

Rachal, D.M., Dello-Russo, R., and Cuba, M., 2024, The Pleistocene footprints are younger than we thought—Correcting the radiocarbon dates of *Ruppia* seeds, Tularosa Basin, New Mexico: Quaternary Research, v. 117, p. 67–78. https://doi.org/10.1017/qua.2023.74

Ritley, K.A., and Odontuya, E., 2004, Yardangs and dome dunes northeast of Tavan Har, Gobi, Mongolia: Geological Society of America Abstracts with Programs, v. 36, no. 4, p 33.

Schenk, C.J., 1990, Eolian deposits of the Ojo Caliente Sandstone Member (Miocene) of the Tesuque Formation, Espanola Basin, New Mexico, *in* Fryberger, S.G., Krystinik L.F., and Shenk, C.J., eds., Modern and Ancient Eolian Deposits—Petroleum Exploration and Production: Rocky Mountain Section–Society of Economic Paleontologists and Mineralogists (Society for Sedimentary Geology), p. 201–209.

Schenk, C.J., and Fryberger, S.G., 1988, Early diagenesis of eolian dune and interdune sands at White Sands, New Mexico: Sedimentary Geology, v. 55, no. 1–2, p. 109–120. https://doi.org/10.1016/0037-0738(88)90092-9

Seager, W.R., Hawley, J.W., Kottlowski, F.E., and Kelley, S.A., 1987, Geology of the east half of Las Cruces and northeast El Paso 1° × 2° sheets, New Mexico: New Mexico Bureau of Mines and Mineral Resources Geologic Map 57, scale 1:125,000, 3 sheets. https://doi.org/10.58799/GM-57

Sebe, K., Csillag, G., Ruszkiczay-Rüdiger, Z., Fodor, L., Thamó-Bozsó, E., Müller, P., and Braucher, R., 2011, Wind erosion under cold climate—A Pleistocene periglacial mega-yardang system in Central Europe (Western Pannonian Basin, Hungary): Geomorphology, v. 134, no. 3–4, p. 470–482. https://doi.org/10.1016/j.geomorph.2011.08.003

Szynkiewicz, A., Moore, C.H., Glamoclija, M., and Pratt, L.M., 2009, Sulfur isotope signatures in gypsiferous sediments of the Estancia and Tularosa Basins as indicators of sulfate sources, hydrological processes, and microbial activity: Geochimica et Cosmochimica Acta, v. 73, no. 20, p. 6162–6186. https://doi.org/10.1016/j.gca.2009.07.009

Szynkiewicz, A., Ewing, R.C., Moore, C.H., Glamoclija, M., Bustos, D., and Pratt, L.M., 2010, Origin of terrestrial gypsum dunes—Implications for Martian gypsum-rich dunes of Olympia Undae: Geomorphology, v. 121, no. 1–2, p. 69–83. https://doi.org/10.1016/j.geomorph.2009.02.017

Talmadge, S.B., 1933, Source and growth of the white sands of New Mexico: Pan-American Geologist, v. 60, p. 304.

Tewes, D.W., and Loope, D.B., 1992, Paleo-yardangs—Wind-scoured desert landforms at the Permo-Triassic unconformity: Sedimentology, v. 39, no. 2, p. 251–261. https://doi.org/10.1111/j.1365-3091.1992.tb01037.x

Urban, T.M., Bennett, M.R., Bustos, D., Manning, S.W., Reynolds, S.C., Belvedere, M., Odess, D., and Santucci, V.L., 2019, 3-D radar imaging unlocks the untapped behavioral and biomechanical archive of Pleistocene ghost tracks: Nature Scientific Reports, v. 9, 16470. https://doi.org/10.1038/s41598-019-52996-8

U.S. Climate Data, 2024, Climate Alamogordo New Mexico and weather averages: https://www.usclimatedata.com/climate/alamogordo/new-mexico/united-states/usnm0002

Wang, J., Xiao, L., Reiss, D., Heisinger, H., Huang, J., Xu, Y., Zhao, J., Xiao, Z., and Komatsu, G., 2018, Geological features and evolution of yardangs in the Qaidam Basin, Tibetan Plateau (NW China)—A terrestrial analogue for Mars: Journal of Geophysical Research–Planets, v. 123, no. 9, p. 2336–2364. https://doi.org/10.1029/2018JE005719

Ward, A.W., 1979, Yardangs on Mars—Evidence of recent wind erosion: Journal of Geophysical Research–Solid Earth, v. 84, no. B14, p. 8147–8166. https://doi.org/10.1029/JB084iB14p08147

Ward, A.W., and Greeley, R., 1984, Evolution of yardangs at Rogers Lake, California: Geological Society of America Bulletin, v. 95, no. 7, p. 829–837. https://doi.org/10.1130/0016-7606(1984)95<829:EOTYAR>2.0.CO;2

Ward, A.W., Doyle, K.B., Helm, P.J., Weisman, M.K., and Witbeck, N.E., 1985, Global map of eolian features on Mars: Journal of Geophysical Research–Solid Earth, v. 90, no. B2, p. 2038–2056 https://doi.org/10.1029/JB090iB02p02038

Weather U.S., 2024, Yearly & monthly weather—Alamogordo, NM: https://www.weather-us.com/en/new-mexico-usa/alamogordo-climate

Whitney, M.I., 1985, Yardangs: Journal of Geological Education, v. 33, no. 2, p. 93–96. https://doi.org/10.5408/0022-1368-33.2.93

Xuemin, G., Zhibao, D., Zhenghu, D., Min, L., Xujia, C., and Li, J., 2019, Wind regime for long-ridge yardangs in the Qaidam Basin, Northwest China: Journal of Arid Land, v. 11, p. 701–712. https://doi.org/10.1007/s40333-019-0108-4

Zhang, D., Wang, G., Pullen, A., Abell, J.T., Ji, J., and Shen, T., 2020, Landscape evolution and development of eolian-modified unconsolidated gravel surfaces and yardangs in the Hami Basin, China: Geomorphology, v. 368, 107355. https://doi.org/10.1016/j.geomorph.2020.107355

Zimbelman, J.R., and Griffin, L.J., 2010, HiRISE images of yardangs and sinuous ridges in the lower member of the Medusae Fossae Formation, Mars: Icarus, v. 205, no. 1, p. 198–210. https://doi.org/10.1016/j.icarus.2009.04.003

Disclaimer:
The data, views, and conclusions included in this report are those of the authors and should not be interpreted as necessarily representing the official policies, either expressed or implied, of the New Mexico Bureau of Geology and Mineral Resources or the State of New Mexico. All data are for informational purposes only, and the user bears all responsibility in determining whether these data are fit for the intended use.

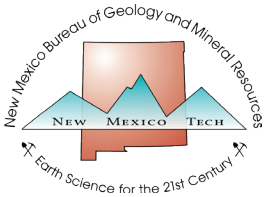

New Mexico Bureau of Geology and Mineral Resources
A research and service division of New Mexico Tech
geoinfo.nmt.edu
801 Leroy Place
Socorro, NM 87801-4796
(575) 835-5490